Nanofibrillar cellulose as a potential reservoir for drug delivery and its application in transdermal drug delivery with the aid of iontophoresis

Mingwei Li
University of Helsinki
Faculty of Pharmacy
Division of Pharmaceutical Biosciences

December 2015

HELSINGIN YLIOPISTO
HELSINGFORS UNIVERSITET
UNIVERSITY OF HELSINKI

Tiedekunta/Osasto Fakultet/Sektion – Faculty	Osasto/Sektion– Department
Pharmacy	Division of Pharmaceutical Biosciences

Tekijä/Författare – Author

Mingwei Li

Työnnimi / Arbetets titel – Title

Nanofibrillar cellulose as a potential reservoir for drug delivery and its application in transdermal drug delivery with the aid of iontophoresis

Oppiaine /Läroämne – Subject

Biopharmacy

Työnlaji/Arbetets art – Level	Aika/Datum – Month and year	Sivumäärä/Sidoantal – Number of pages
Master's thesis	December 2015	65 (+ appendices)

Tiivistelmä/Referat – Abstract

Nanofibrillar cellulose (NFC) can form hydrogels with high water content (> 98 %). It has been studied for drug release, and it has been used as a cell culture matrix, due to its similar structure to extracellular matrix (ECM). In addition it has been found that they has no cytotoxicity. Iontophoresis is the application of an electric current over a defined area for the purpose of enhancing permeation across a membrane for ionized drug species.

The aim in the experimental work in this Master's thesis is twofold. First, to find out the suitable drug loading concentrations into NFC hydrogels, which can provide a good release profile, a release study with two model drugs, propranolol and ketoprofen, loaded into three types of NFC hydrogels at three different concentrations, was carried out for this purpose. Second, to see if NFC hydrogels are applicable as a drug reservoir in iontophoretic transdermal drug delivery applications, an iontophoresis study was carried out using porcine ear skin model *in vitro* for human skin with propranolol loaded into NFC hydrogel of type A. In addition, Stella models were used as an aid to find suitable ways to predict the release and permeation behaviour of models drugs in the abovementioned context.

The UPLC results from the release study show for both model drugs, the wt. % released had linear correlation with squareroot of time. At 6 hours, more than 70 wt. % propranolol was released from hydrogel reservoir. For ketoprofen, the release varied between 30 – 87 wt. %, where higher initial loading concentrations produced a decrease in the wt. % released from hydrogel. The iontophoresis study did not show a significant difference between the tested current densities (0.50 mA/cm^2; 0.25 mA/cm^2) produced on the wt. % of drug released. Simulation models could be run with the mathematical equations for diffusion controlled drug release. In conclusion, the NFC hydrogels show potential as drug reservoir for drug release. Additional experimental data using other types of drug reservoirs should be obtained for a better understanding of the suitability of NFC hydrogels as a drug reservoir in iontophoretic transdermal drug delivery.

Avainsanat – Nyckelord – Keywords
nanofibrillar cellulose, drug reservoir, diffusion, controlled release, iontophoresis, skin

Säilytyspaikka – Förvaringställe – Where deposited
Division of Pharmaceutical Biosciences

Muitatietoja – Ovriga uppgifter – Additional information
Supervisors: Prof. Marjo Yliperttula, Docent Timo Laaksonen

HELSINGIN YLIOPISTO
HELSINGFORS UNIVERSITET
UNIVERSITY OF HELSINKI

Tiedekunta/Osasto Fakultet/Sektion – Faculty	Osasto/Sektion– Department	
Farmasia	Farmaseuttisten biotieteiden osasto	
Tekijä/Författare – Author		
Mingwei Li		
Työnnimi / Arbetets titel – Title		
Nanofibrillaarinen selluloosa potentiaalisena varastona lääkeannostelussa ja sen soveltaminen transdermaalisessa lääkeannostelussa iontoforeesin avulla		
Oppiaine /Läroämne – Subject		
Biofarmasia		
Työnlaji/Arbetets art – Level	Aika/Datum – Month and year	Sivumäärä/Sidoantal – Number of pages
Pro Gradu	Joulukuu 2015	65 (+liitteet)

Tiivistelmä/Referat – Abstract

Nanofibrillaarinen selluloosa (NFC) voi muodostaa hydrogeelejä, joissa on korkea vesipitoisuus (> 98 %). Sitä on tutkittu lääkeannostelussa, ja sitä on käytetty solukasvatusmatriisina, koska siinä on samankaltainen rakenne kuin soluväliaineessa. Tämän lisäksi on havaittu, ettei sillä ole sytotoksisuutta. Iontoforeesi on sähkövirran käyttö tietyllä pinta-alalla, minkä tarkoitus on lisätä ionisoituneen lääkeaineen permeaatiota kalvon läpi.

Tämän Pro Gradu –tutkielman tavoite on kaksiosainen. Ensiksi, jotta löytyisi sopivat lääkelatauspitoisuudet NFC hydrogeeleihin, joilla saavutetaan hyvä vapautumisprofiili, tehtiin vapautumiskoe kahdella mallilääkeaineella, propranololilla ja ketoprofeenilla, jotka ladattiin NFC hydrogeeleihin kolmessa eri pitoisuudessa, tätä tarkoitusta varten. Toiseksi, jotta näkisi, ovatko NFC hydrogeelit sovellettavissa lääkevarastona iontoforeettisessa transdermaalisessa lääkeannostelusovelluksissa, toteutettiin iontoforeesikoe *in vitro* ihmisihoa edustavalla siankorvan ihomallilla, käyttäen propranololia ladattuna NFC hydrogeeli tyyppi A. Lisäksi, Stella-malleja käytettiin apuna yrityksessä löytää tapoja ennustaa mallilääkeaineiden vapautumis- ja permeaatiokäyttäytymistä yllämainitussa kontekstissa.

Vapautumiskokeesta saatujen UPLC tulosten perusteella, vapautumisprosentilla (wt. %) on suora korrelaatio ajan neliöjuuren suhteen. 6 tunnin kohdalla, yli 70 wt. % propranololia oli vapautunut hydrogeelivarastosta. Ketoprofeenin vapautuminen vaihteli välillä 30 – 87 wt. %, ja korkeammat alkulatauspitoisuudet saivat aikaan hydrogeelistä vapautuneen osuuden (wt. %) pienentymään. Iontoforeesikokeessa ei käynyt ilmi, että kahden testatun virrantiheyden (0.50 mA/cm^2; 0.25 mA/cm^2) välillä olisi merkittävää eroa aiheutunut vapautuneeseen lääkeosuuteen wt. %). Oli mahdollista ajaa simulaatiomalleja diffuusiorajoitteista lääkevapautumista kuvaavien matemaattisten yhtälöiden avulla. Thteenvetona, NFC hydrogeeleillä on potentiaalia lääkevarastona lääkevapautumiselle. Lisää kokeellista dataa, joissa käytetään muuntyyppisiä lääkevarastoja tulisi saada, jotta olisi mahdollista ymmärtää paremmin NFC hydrogeelien soveltuvuutta lääkevarastona iontoforeettisessa transdermaalisessa lääkeannostelussa.

Avainsanat – Nyckelord – Keywords
nanofibrillaarinen selluloosa, lääkevarasto, diffuusio, hallittu vapautuminen, iontoforeesi, iho

Säilytyspaikka – Förvaringställe – Where deposited
Farmaseuttisten biotieteiden osasto

Muitatietoja – Ovriga uppgifter – Additional information
Ohjaajat: Prof. Marjo Yliperttula, Dosentti Timo Laaksonen

Table of Contents

Appendices

LITERATURE REVIEW

1. Introduction

A transdermal drug delivery system focuses on drug delivery through the skin. Iontophoresis is one possible method of transdermal drug delivery, which requires the application of an electric current onto the target membrane, which is to be permeated by the drug.

One of the goals in iontophoretic drug delivery is to obtain freedom of adjusting the most suitable dose necessary at a given time. It is also a possible key to personalized medication. For iontophoresis, the transdermal route of drug delivery is very appealing. The skin is easily accessed and the area of possible sites of administration is large. In addition the skin can renew itself.

Iontophoresis has been investigated as a way to overcome the skin barrier that prevents drug delivery into systemic circulation (Kalia et al. 2004). Iontophoresis is considered to offer different advantages over administration by injection, because the type of damage on and into the skin is less invasive (van der Geest et al. 1996). Compared with drug administration by injection, where pain and bruising at the site of injection is common, the iontophoretic transdermal delivery can offer a gentler alternative.

In transdermal delivery, there is always a drug reservoir requirement, especially if extended and even drug release is to be contained. Therefore a proper material must be selected. One of the potential material is nanofibrillar cellulose, which can form hydrogels with a high water content.

In addition, by coupling iontophoretic drug delivery with a suitable hydrogel drug reservoir, more defined controlled over the drug administration could be possibly achieved and

controlled drug delivery realized through control of the level of electric current applied. Because iontophoretic drug delivery offers enhanced diffusion of the drug molecule across the skin, it is important to be able to control that the drug storage is reliable and does not cause sudden release of the drug in reservoir due to a storage material damage, such as deterioration or sudden rupture.

In this MSc (Pharm.) thesis, the literature review covers an overview on the properties of skin from the point of view of requirements of iontophoresis, properties of nanofibrillar cellulose (NFC) and NFC hydrogel, and iontophoresis as a method for transdermal drug delivery. The iontophoresis is chosen as a point of focus, since the NFC hydrogels chosen for the experimental part have not been tested in iontophoretic applications before. The experimental part consists of a release study and an iontophoresis study. In addition, Stella models are built based on experimental results.

2. Transdermal drug delivery

Transdermal drug delivery refers to the administration of drug through the skin. The desired effect can be either system or the local. A transdermal drug delivery system is commonly regarded as a controlled drug delivery system (Wiedersberg and Guy, 2014).

For a drug effect to occur in the body and a desired response to be induced, a certain level of drug must be present in the body at the desired site of action (Rowland and Tozer, 2011). It is known that often a certain level of drug concentration in plasma can be measured, before a desired effect of drug in the body can be triggered. Therefore a controlled drug delivery system is a way to maintain the optimal level of drug in the body over a chosen period of time. The time period in controlled drug delivery can be short or extended.

There are many different types of drug administration route that uses the skin as a site of assess. For example, injection based drug formulations pass through the skin through the

aid of the needle and the level of penetration is high and most likely causes some bleeding. The conventional syringe based injection-type of transdermal drug delivery is out of scope of this work.

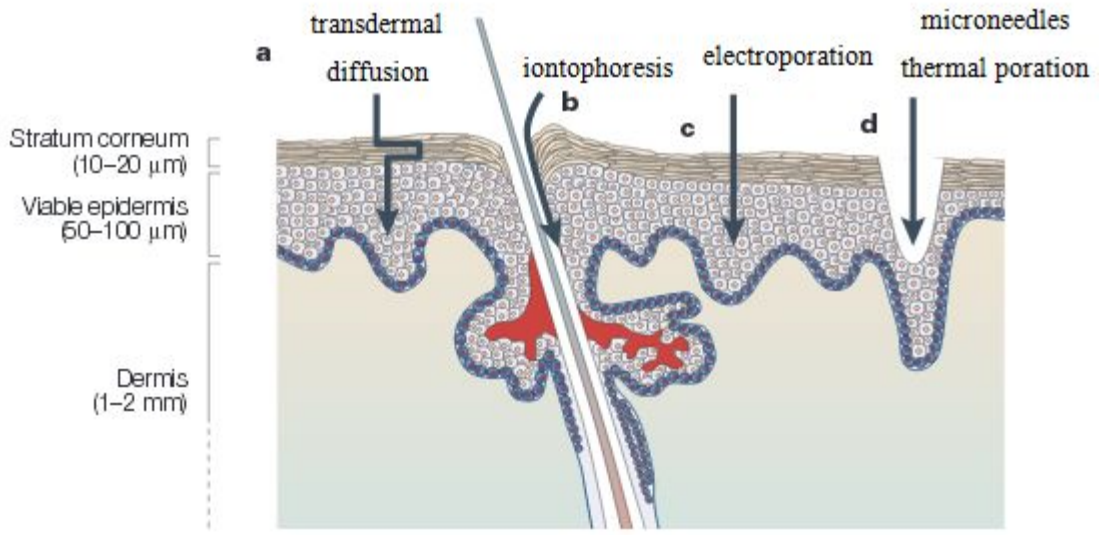

Figure 1. Structure of the skin and possible pathways of transdermal drug delivery (modified from Prausnitz et al. 2004)). 1a. Transdermal diffusion. 1b. Iontophoresis. 1c. Electroporation. 1d. Microneedles or thermal poration.

There exists several options for the delivery mechanism in transdermal drug delivery. It should noted that all the presented transdermal drug delivery options presented in figure 1 help the drug pass through *stratum corneum*. In addition to iontophoresis, there exist microneedling and electroporation among others (Arora et al. 2008). The use of microneedles in transdermal drug delivery was first studied 17 years ago by Henry and coworkers (1998). In the study, they described that the target site of the microneedles was just beyond stratum corneum, since going deeper can possible cause nerves in the viable epidermis to be stimulated, which can result in a sense of pain. In the study, they observed that a higher permeability of the skin was achieved when the microneedles were removed after puncture than letting the microneedles stay in the skin. The microneedles used was 150 μm in length and left a hole of ~1 μm.

Both iontophoresis and electroporation require the use of an electric current. Iontophoresis causes a low-voltage electrical enhancement while electroporation causes a high-voltage enhancement (Prausnitz et al. 2004). The focus in this work is on iontophoresis as a method of transdermal drug delivery. The most obvious advantage of this route of drug delivery is that first-pass metabolism by the liver can be avoided (Rowland and Tozer, 2011).

3. Iontophoresis on skin

Iontophoresis in transdermal drug delivery requires the application of a electric current over a defined area on the skin. The iontophoretic flux can be expressed as the sum of electromigration and electroosmosis (Kalia et al. 2004). In electromigration, the ions move due to the created electric field, while electroosmosis can be understood as a flow of charge through the skin. In addition to the skin, other possible sites for iontophoretic drug administration include buccal mucosa (Gratieri and Kalia, 2014) and sclera of the eye (Tratta et al. 2014). The aim of using iontophoresis is to enhance the permeability of an ionized drug species through skin.

A proper understanding of the skin physiology is important in order to avoid those types of possible damage on the skin, which might affect the administration of the drug through iontophoresis. Especially, since the ideal goal in iontophoretic drug administration is to be able to adjust the dose through the control of current density applied, it is necessary to be able to know what kind of frequency of dosing is applicable without causing disturbing changes at the site of adminstration.

There is a limit in the range of possible current densities, which can be applied to the skin. The upper limit of the acceptable current density for human use is often set at 0.5 mA/cm^2, and furthermore, both perception and pain thresholds should be considered (Prausnitz, 1996). Ideally, within this range of applicable current densities, there may exist possibility

to induce clinically relevant dose administration through skin. In addition, there is a possibility choosing between continuous or pulsed iontophoresis. However, the benefits of pulsed iontophoresis over continuous iontophoresis remain unclear (Kotzki et al. 2015).

Of course, unless there is fixed area in a defined position in the body possessing optimal skin properties that are good for drug administration of a specific drug, one can change the areas of skin, where the current is applied. It should be noted that the drug dose permeating through can be readily enhanced by a simple increase of the area exposed (Kalia et al. 2004).

The formulation of the drug vehicle has many possibilities. It has been shown that it is possible to load peptides onto nanogels and then apply iontophoresis for transdermal drug delivery (Toyoda et al. 2015). Also, the way iontophoresis is applied has alternatives. For example, iontophoretic skin patches can be used with anode and cathode electrodes built-in in the patch (Saluja et al. 2013). Furthermore, the possibility of adding permeability enhancing agents should not be forgotten. It has been reported that the addition of oleic acid into propylene glycol vehicle with donepezil base, or palmitoleic acid into propylene glycol vehicle with donepezil hydrochloride salt, can enhance the permeability of both forms of donepezil across hairless mouse skin in *in vitro* conditions without iontophoresis (Choi et al. 2012).

The effect of Na^- concentration on iontophoretic flux (J_{ss}) has been studied previously by Malinovskaja and coworkers (2013). They observed that 15.4 mM Na^- concentration has proven to be optimal for the highest J_{ss} value and transport number

Due to the less invasive nature of iontophoresis aided transdermal drug delivery when compared to conventional syringe based injections, iontophoresis has potential as an alterative to injections, especially in the field of paediatrics (Delgado-Charro and Guy, 2014).

4. Properties of the skin

The skin, like other tissues, is anisotropic (Grimnes and Martinsen, 2000). Therefore, when consideration is done concerning the drug delivery applications, the layers of skin and their orientation should be considered.

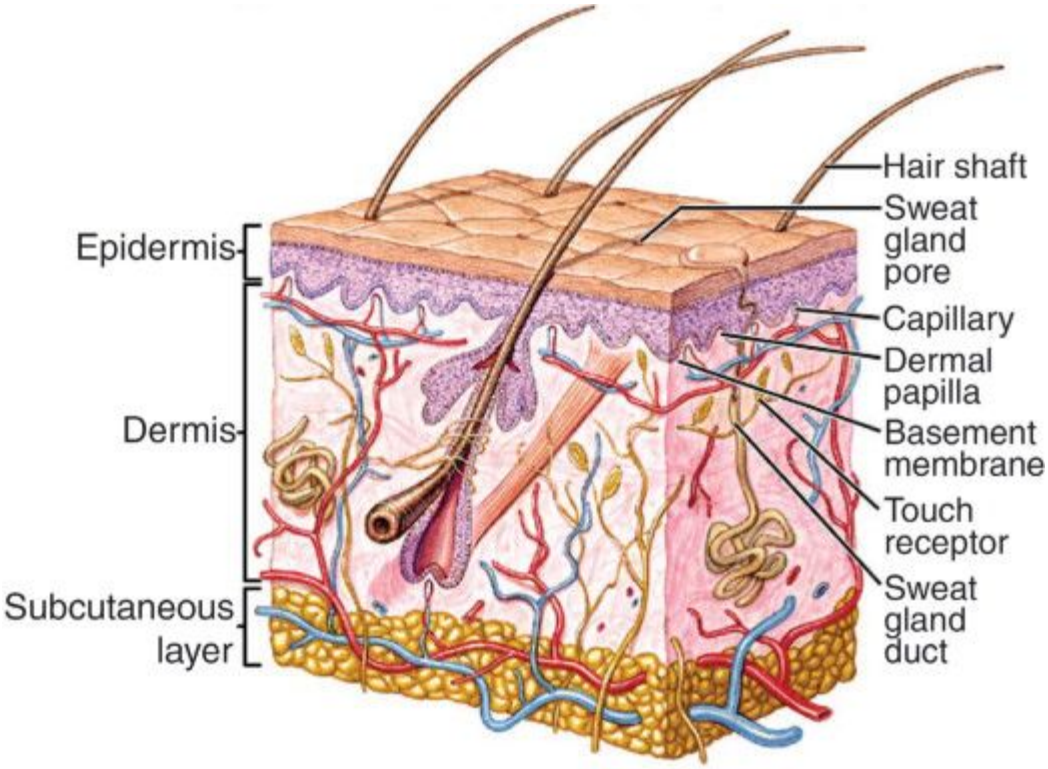

Figure 2. Structure of human skin (MacNeil, 2008).

4.1. Stratum corneum

The epidermis (figure 2) contains two parts: *stratum corneum* and viable epidermis (Geerligs et al. 2011). The *stratum corneum* is well-formed barrier that protects the human body. It is composed of dead corneocyte layers, which range between 10-15 layers to form the *stratum corneum* (Badiu et al. 2009). On the surface of the *stratum corneum*, there

exists a corneocyte lipid envelope (CLE), which consists of ω-hydroxyceramides (Elias et al. 2014).

For the maintainance of normal properties of *stratum corneum*, on the surface of corneocytes, the corneodesmosomes undergo regulated remodeling (Kitajima 2015). The enzymes that participate in the ceramide formation and degradation must meet sufficient levels of enzyme activity in order to maintain a healthy *stratum corneum* (Choi and Maibach, 2005).

The *stratum corneum* has a thickness of 10-20 μm and a major role in the prevention of transepidermal water loss (TEWL) (Bouwstra et al. 2003). Recently, it has been suggested that the resistance to TEWL in the *stratum corneum* is depth-dependent and a different resistance profile can be assigned to each section (top, middle, bottom) of *stratum corneum* (van Logtestijn et al. 2015).

The properties of the human *stratum corneum* vary depending the gender and the age. The normal water content of the *stratum corneum* is about 20 % (w/w) (Bouwstra et al. 2003). There exists evidence that the *stratum corneum* becomes stiffer and the cellular cohesion increases when the age of the owner of the skin advances (Biniek et al. 2015). In contrast, since the *stratum corneum* starts to develop only at the seventh month of a pregrancy, the skin of a preterm infant can absorb readily high amounts of a substance, such as methylated spirits, that is in contact with the skin into its blood stream (Harpin and Rutter, 1982).

In a study with 300 subjects (female and male, age between 20-74), it was revealed that TEWL on forearm skin is always greater in females than in males (Luebberding et al. 2013). In the same study, it was also found out that the sebum production on the cheek was higher in males than females within all age groups. Additionally, the pH value of the skin is below 5 for males and over 5 for female, with minor exceptions (e.g. forehead) for the latter.

As more developed ways of visualization became available, it has been realized that the *stratum corneum* is a highly organized living material with a complex metabolic activity owning to a diverse types of cells, which maintain its physical, chemical and enzymatic barrier function (Menon et al. 2012). The common parts that *stratum corneum* is comprised of include corneocytes, corneodesmosomes, lamellar bodies, various lipids, and enzymes that have lipolytic and proteolytic activity. It is possible to study the structure of the intercellular lipid matrix in the *stratum corneum* using Raman spectroscopy (Kikuchi et al. 2015). The major advantages in Raman spectroscopy is the noninvasiveness of the method, while still providing high quality details and spatial resolution (Caspers et al. 2001). Therefore, the noninvasive nature of the Raman spectroscopy makes it ideal for *in vivo* analysis of superficial skin structure.

It is important to understand that although the *stratum corneum* comprises of cells that are no longer viable, it still contains in itself a considerable amount of possible pathways for metabolic responses in addition to its adaptability against enviromental changes such as temperature and humidity.

Recently, it has been studied in depth, that the topographical features of the *stratum corneum* affect both the magnitude and the location of the applied strain on skin (Leyva-Mendivil et al. 2015). The study in question used 2D imaging and literature data to perform the computational study. They divided the *stratum corneum* to different types of regions based on the crests and furrows that appeared on it. The study found out that the *stratum corneum* is capable of alleviating the strain applied to not only itself, but also to epidermis and dermis. This indicates that if the condition of the *stratum corneum* is altered, such as humidity or dryness, the underlaying layers of skin will also be influenced, since the *stratum corneum* cannot then react properly against the strain.

Regarding the mechanical properties of the skin, it is known that *stratum corneum* and viable epidermis possess comparable stiffness, with a value in the range of 1-2 Mpa when loaded perpendicularly (Geerligs et al. 2011). Concerning the blood flow at the skin depth,

there exist one horizontal plexus at a depth of 1-1.5 mm from skin surface and another at the interface of dermal and subcutaneous layers of the skin (Braverman 2000). In addition, there are no blood vessels in the epidermal layer of the skin (Liao et al. 2013).

Based on the above information on the skin and its blood flow, it is certain that for a drug to enter into the systemic circulation by transdermal administration, it must pass through the epidermal layers until the dermal layers containing blood flow are reached. Since it is common that the iontophoretic transdermal drug delivery aims beyond local administration, it is important that this can be achieved.

Based on the fact that *stratum corneum* topography, skin depth and blood flow differ in different parts of the body, it is necessary to establish, to what this extent these variations influence iontophoresis and then further determine, if these effects are significant in the context of iontophoretic drug administration.

4.2. Considerations on pH and pI of skin

A study done using dermatomed skin of 750 µm showed that lysozyme electrotransport had decreased cumulative permeation when the pH (5, 6, and 7.15) of the formulation rose further from the skin isoelectric point (pI ~4.5), and study concluded that when pH > pI, the increased ionization of negatively charged groups in the skin will decrease electrotransportation (Dubey and Kalia, 2014). In addition, it is thought that ionized carboxylate groups create conditions for the cation permselectivity of the skin, since the ions move towards the direction, which results in neutralizing the existing charge difference (Kalia et al. 2004).

Both the pH of a drug formulation and the possible interactions of the drug with the *stratum corneum* can affect the permeability of a drug during iontophoresis (Dubey and Kalia, 2014). It should be noted that the pH of the donor buffer solution can alter both drug permeability and the pH of *stratum corneum* itself (Oshizaka et al. 2014).

The study by Oshizaka and coworkers (2014) showed that after a drug permeation experiment, the *stratum corneum* on full-thickness skin could keep its pH close to its original pH of 6.2, when the donor buffer solution had a pH of 5.0 or 7.4. However, when the donor buffer solution had a pH value of 10.0, the pH of the *stratum corneum* after the experiment increased to pH 8.8. The viable epidermis and dermis keep their original pH values after experiment better than the *stratum corneum* under different donor buffer solutions, most likely due to the fact that they are in deeper parts of the skin and get protection from *stratum corneum*.

4.3. Effect of iontophoresis on skin

The priority in iontophoresis is to direct and influence the flow of ionic species (Kalia et al. 2004). However, it is commonly known that skin reactions appear after the application of current on the skin (Curdy et al. 2001).

For example, the effects induced by iontophoretic current on forearm skin of human volunteers has been studied using $Ag^+/AgCl$ electrodes with exposed skin area being 2.5 cm^2 (van der Geest et al. 1996). Both transepidermal water loss (TEWL) and erythematous response were measured and evaluated after a 30 min application of either continuous (0.25 mA/cm^2) or pulsatile (0.50 mA/cm^2) current. The results show that TEWL values were elevated during current application and returned to baseline level in 30-45 min after removal of the iontophoretic device. The erythematous response was assessed by measuring the cutaneous blood flow using Laser Doppler Flowmetry (LDF) and also a visual score was given to the degree of skin reaction. It was observed that current direction plays a role: under the anode, the response was higher than under the cathode. In addition, at anode the duration of the response lasted longer than at cathodal site.

It has been established that iontophoresis can alter the microvascular blood flow under the skin (Tesselaar and Sjöberg 2011). In addition, it is known that the ethnic origin of the skin

can affect the TEWL of the skin (Wesley and Maibach 2003). However, it should be understood that these parameters are only required to be controlled locally, when necessary.

5. Effects of iontophoresis on transdermal drug delivery

5.1. Effects on drug permebility and deposistion

Iontophoresis may be applied to both small molecule drugs and larger compounds with high molecular weight. It has been demonstrated that iontophoresis can enhance the drug accumulation of acyclovir through skin at a depth of 200-350 µm below skin surface, when the pH was 3.0 (Volpato et al. 1998). As for larger compounds, it is possible for iontophoresis to enhance the cumulative permeability of RNAse T1, which is a negatively charged protein with a molecular weight of 11.1 kDa (Dubey and Kalia 2011). Furthermore, in the same study, the skin deposition of the protein was not influenced by the application of different degrees of current density.

Based on the above information from the study (Dubey and Kalia 2011), it seems that there is no rate-limiting accumulation of the drug formed on the skin and therefore the drug will swiftly pass further into the skin layers.

5.2. Types of drugs used in the iontophoretic transdermal drug delivery

The iontophoretic transdermal delivery is suitable for drugs, which are meant for the treatment of chronic diseases, where a good treatment balance can be achieved by the adjustments of dosing within a predetermined safe dose range, based on the conditions of symptoms or the condition of the patient.

In general, lipophillic and potent drugs with a M_w under ~ 400 Da, such as fentanyl and estradiol, have had great success in transdermal drug delivery (Wiedersberg and Guy 2014).

The iontophoresis has an option of enhancing the permeation of these drugs or expanding the selection of drugs suitable for transdermal drug delivery. Both small molecule drugs, such as apomorphine (Malinovskaja et al. 2013), and protein drugs, such as leuprorelin (Malinovskaja et al. 2014), can achieve higher permeability through skin by using iontophoresis.

It is common knowledge that a good formulation can always help a drug with otherwise difficult characteristics, such as poor solubility. Therefore, the formulation should be always considered in conjunction with the selection of suitable drugs chosen for this route of delivery.

6. Porcine ear skin as a model for human skin

It is generally well-known that the porcine ear skin is a good representative substitute for human skin (Jacobi et al. 2007). In a study by Jacobi and coworkers (2007), the measured thickness of *stratum corneum* and viable epidermis were 17-28 µm and 60-85 µm, respectively. The thickness of porcine *stratum corneum* is therefore comparable with the thickness of human *stratum corneum*. An apparent thickness of *stratum corneum* in human (*in vivo*) and in porcine ear skin (*ex vivo*) has been reported to be 11.7 ± 3.2 µm and 8.5 ± 3.0 µm, respectively, in another study (Herkenne et al. 2006). Furthermore, it has been been shown that porcine skin has similar pI value (4.4) and shows similar cation permselectivity as human skin (Marro et al. 2001).

Concerning the enzyme activity on the surface of the skin, it has been confirmed that esterases exist both on the *stratum corneum* and the epidermis of the porcine ear skin (Lau et al. 2012). For *stratum corneum*, the presence of esterases in skin samples frozen at -20 °C for a week is comparable to the amount of esterases present in freshly excised samples, based on the histochemical staining.

There is also a possibility to use only a portion of porcine skin. Tape stripping is a common method employed to study how the barrier effect changed, when layers are removed from the surface of the skin (Dubey and Kalia 2014). In addition it is also used to obtained dermatomed skin. In tape stripping the layers of skin obtained is partial. Tape stripping done to porcine skin can be used as a substitute for tape stripping done on human skin, when studying how the a drug compound penetrates into the uppermost skin layers (Klang et al. 2012).

Since tape stripping does not provide full-thickness skin, it is not suitable for iontophoretic permeability studies, where the target site is the blood flow beyond the skin surface, when a systemic effect is desired.

7. Nanofibrillar cellulose (NFC) and NFC hydrogels as a storage for drug release

In general, when selecting a suitable hydrogel for a controlled release formulation, one basic consideration is the identification of the rate-limiting step in the controlled release system, after which the drug release mechanism is categorized as diffusion, swelling or chemically controlled (Lin and Metters 2006). There are hydrogels that swell in water and others that do not. Cross-linking prevents the hydrogel from dissolving into water (Saltzman 2001). A swelling response of a hydrogel can be induced by changing the surrounding pH condition, which causes increased ionic repulsion among the ionic groups present in the gel (Das and Subuddhi 2015). Chemical control is often related to enzymatic degradation of a hydrogel matrix (Lin and Metters 2006). In contrast to the swelling and checmically controlled drug release formulations, which use less stable hydrogels have the ability to change based on environmental cues, the diffusion controlled drug release may gain benefit by choosing a more stable hydrogel material, such as the nanofibrillar cellulose, which will be discussed in further detail below.

7.1. Properties of nanofibrillar cellulose (NFC)

The naming convention for different types of nanocelluloses has not always been used in a consistent manner, which has resulted in several names for nanofibrillar cellulose, such as microfibrillated cellulose, nanofibrillated cellulose and nanofibrils (Klemm et al. 2011). Another term that can be used is cellulose nanofibril (CNF) (Sacui et al. 2014).

Nanofibrillar cellulose (NFC) is a type of cellulose that can be obtained from various including trees and bacteria. The origin of the nanofibrillar cellulose affect its fiber diameter and for example, in birch originated TEMPO-oxidized NFC its fiber diameter is within 3-5 nm (Valo et al. 2013). The NFC is considered to have a high aspect ratio, with a diameter of 5-60 nm, while its length can reach up to several micrometers (Klemm et al. 2011).

Although the mechanical treatment is the predominant process in obtaining NFC, additional steps such as chemical or enzymatic pre-treatment may be added in the process, based on the choice of raw material and the desired level of modification (Siró and Plackett 2010).

The surface chemistry of the nanofibrillar cellulose vary depending the hydrolysis technique applied. Mechanically refined wood pulp yields NFC with hydroxyl (neutral) surface chemistry, while after TEMPO-mediated oxidation, the resulting NFC has carboxylate (negatively charged) surface chemistry (Sacui et al. 2014). Recently, it has been demonstrated that bromide-free alkali pretreatment can enhance the control over the extent of oxidation during the production of TEMPO-oxidized NFC (Pönni et al. 2014). The bromide-free TEMPO-oxidation is considered to be more friendly to the environment (Bragd et al. 2000).

It is known that the presence of counterions in TEMPO-oxidized nanofibrillated cellulose (NFC) can impact further network swelling, depending on the type of counterion present (Maloney 2015). The results from a study by Maloney (2015) show that highest swelling,

3.6 mL g^{-1}, in NFC occurred when Na^{+} was used as the counterion, while Ca^{2+} caused lowest swelling with a value of 2.1 mL g^{-1}. The study also showed that the network swelling is defined as the sum of intraparticle and interparticle swelling. It should be noted that the immobilized water present between the nanocellulose fibrils are also included in swelling measurements.

Nanofibrillar cellulose has both amorphous and crystalline regions (Valo et al. 2013). It is known that depending on the source of origin, the crystallinity of the NFC can vary (Sacui et al. 2014). One major difference between nanofibrillar cellulose and nanocrystalline cellulose is the fact that the amorphous sections of the cellulose are removed from the latter (Klemm et al. 2011).

7.2. Properties of NFC hydrogel

The NFC hydrogel refers to hydrogels containing NFC and water.The most abundant width of nanofibrillar cellulose (NFC) hydrogel is 20-30 nm, while the smallest diameter of a single fiber is 7 nm (Bhattacharya et al. 2012).

The NFC hydrogel exhibits reversible gelation and the gel strength of NFC hydrogel can well resist a change over a broad temperature and pH range, due to the alignment of its macromolecules (Bhattacharya et al. 2012). Furthermore, it is known that drugs bind to the NFC hydrogel based material itself, and pH and electrostatic forces are thought to be causing a major impact in this process (Kolakovic et al. 2013). It is possible to archieve a sustained release of poorly water soluble drugs from a film reservoir, which is made from NFC hydrogel, up to 90 days (Kolakovic et al. 2012).

The NFC hydrogel has found novel application as a cell culture matrix. It has been shown that human pluripotent stem cells (hPSCs) can grow and form into 3D spheroids of 100-250 μm when the concentration of the NFC hydrogel is suitable, that is at 0.5 wt.%. (Lou et al. 2014). In addition, NFC hydrogel has also been found to have no cytotoxicity and its

structure has similarities with extracellular matrix, which is normally surrounding the cells in their natural enviroment (Bhattacharya et al. 2012).

8. Conclusions from literary review

It should be considered that the formulation used for iontophoresis does not need to be the most simple one possible. The enhanced penetration of a drug induced by iontophoresis can be possibly further improved through an addition of a vasodilative or blood-flow inducing agent. It should be noted however that the choice for the most suitable enhancement agent may need to be carefully made, since a different form of the drug may need a different enhancement agent, as shown in the example of donepezil skin permeability enhancement with fatty acids.

Although in iontophoretic drug delivery the blood flow is a target site of administration, the possibility of the epidermal skin layers acting as a temporary site of storage for the drug, should not be excluded. The reasoning is that it is not known how far the permeability of a specified drug into the skin layers can be enhanced without compromising other aspects, such as the recovery of the skin.

As with the general trend of going towards the individualized treatment of diseases, the undesired effects of iontophoresis on skin can be minimized by pre-testing the patients for the selected properties of the skin in order to evaluate the suitability of the skin condition for the iontophoretic treatment and adjust the dose to a proper level before the drug treatment is initiated. One of the pre-testing for the structure of skin could be done using Raman spectroscopy, which could be done *in vivo* noninvasively.

The lack of cytotoxicity makes the NFC hydrogel a good option for transdermal drug delivery. In addition, the source of the NFC hydrogel is abundant, with many types of

modifications available for the optimization of NFC based hydrogels and materials for a more specific need, such as extended release.

9. Aims of the study

The aim in the experimental work in this Master's thesis is twofold. First, to find out the suitable drug loading concentrations into NFC hydrogels, which can provide a good release profile, a release study with two model drugs, propranolol and ketoprofen, loaded into three types of NFC hydrogels at three different concentrations, was carried out for this purpose. The aim here is to evaluate the suitability of NFC hydrogels as a drug release reservoir.

Second, to see if NFC hydrogels are applicable as a drug reservoir in iontophoretic transdermal drug delivery applications, an iontophoresis study was carried out using an *in vitro* porcine ear skin model for human skin with propranolol loaded into NFC hydrogel of a native type. The aim here is to evaluate if a change in the applied current density can influence the amount of drug, which permeates through the skin. In addition, Stella (isee systems) models were built as an aid to find suitable ways to predict the release and permeation behaviour of models drugs in the abovementioned context.

EXPERIMENTAL PART

10. Materials and Methods

10.1. Drug loaded nanofibrillar cellulose (NFC) hydrogel

Three different nanofibrillar cellulose (NFC) hydrogels (A, B and C) were used in the drug release studies, hereafter simply called also gel. For the iontophoresis study, gel A was used. All of the hydrogels were manufactured and kindly donated by UPM-Kymmene Corporation, Finland. The NFC hydrogels chosen for the experimental part do not rely on swelling or chemical cues to achieve controlled release of the drug. The drug release is assumed to happen based on diffusion controlled drug delivery mechanism.

The nanofibrillar cellulose (NFC) hydrogels chosen for the experimental part possess a high water content (>98 %). They uptake their share of water and then no further swelling occurs when getting into contact with water. Gel A had received mechanical treatment only and its NFC concentration is 1.65 % (w/v). Anionic gel B and gel C had gone through TEMPO-oxidation and their concentrations were 1.16 % (w/v) and 1.5 % (w/v), respectively. The pH values of the NFC hydrogels used in the release study and iontophoresis study were measured as a part of the experimental work and they are presented in the Results section (11.1 pH of the NFC hydrogels) of this work.

For our purposes, the method of preparation was kept as simple and straightforward as possible and the gel was only loaded with the desired amount of drug and a necessary amount NaCl. The gel was kept as unmodified as possible.

The drug loaded gels were prepared by hand and only solid form drug and NaCl were added. Three drug concentrations was prepared for each gel: 10 mg/g, 30 mg/g and 90 mg/g. The drug loaded gels become matrix type hydrogels, where the drug is uniformly mixed with the gel. The matrix type is easy to handle, since there are no additional restrictions on the orientation of the gel when depositing it onto the experimental donor compartment, namely a septum cap.

Most often, 5 g of gel was prepared for each concentration. For each 5 g of gel, 4.5 mg of NaCl was used in addition to the required amount of drug for each concentration. This was done to obtain a 0.09 % NaCl concentration in gel. The NaCl concentration was chosen to be less than the isotonic 0.9 % concentration, since the amount of competitive co-ions were kept in minimum, in order to achieve higher fluxes under iontophoresis (Malinovskaja et al. 2013).

Mixing was done after all the ingredients were applied into a glass bottle. A syringe (1 ml) was used to mix the loaded gel for 10 min. Before mixing, the content was shaken to let the solid drug get into better contact with the gel. Each prepared gel was stored in a refrigerator (+2 – +8 °C) located in the laboratory. They were stored in sealed bottles, which were parafilm wrapped to further ensure the prevention of dehydration.

It can be observed from figure 3 that in freshly made batches of loaded gel, the ketoprofen loaded gel A is opaque white, since ketoprofen does not dissolve into the gel A almost at all. In contrast, the propranolol has a degree of translucency and its appearance resembles the unloaded gel A. Two lighting conditions were used for the photos for a better contrast and comparison.

Figure 3. Gel A loaded with ketoprofen (30 mg/g, left) and propranolol (30 mg/g, right). Photos from the experimental study with two different lighting conditions. The ketoprofen loaded gel contains solid ketoprofen, which does not dissolve into the gel well.

10.2. Model drugs used

In the experimental part, two drug compounds were used. (±)- Propranolol hydrochloride was obtained from Sigma-Aldrich (Schnelldorf, Germany). Ketoprofen was obtained from Orion (Espoo, Finland).

We chose propranolol and ketoprofen, since they have opposite charges at physiological pH 7.4. Propranolol has a pKa value of 9.42 (DrugBank 2013b). The pKa value for ketoprofen is 4.45 (DrugBank 2013a). Based on the chemical structures, it can be seen that propanolol is a weak base and ketoprofen is a weak acid (figure 4). Therefore, at physiological pH 7.4, both drugs are in ionized form: the propranolol is in cationic form and ketoprofen is in anionic form. Therefore, we use propranolol as a model drug for a cationic drug species, and ketoprofen acts as a model drug for an anionic drug species.

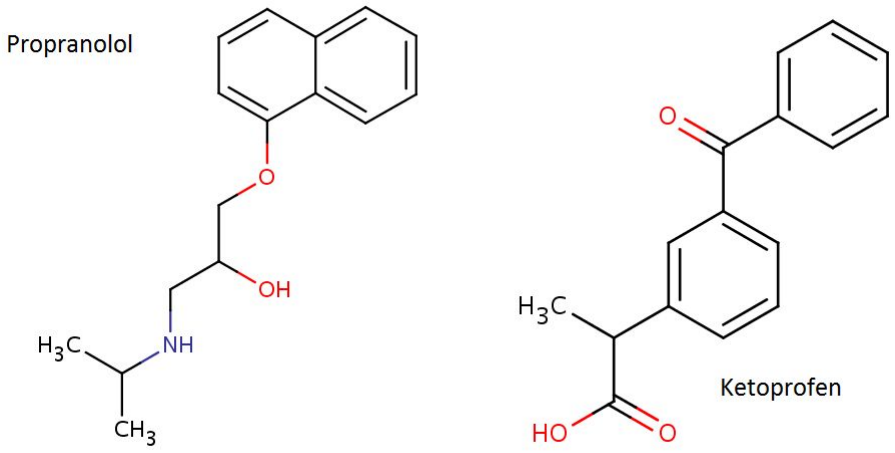

Figure 4. The chemical structures of propranolol and ketoprofen (DrugBank, 2013a, 2013b).

Both propranolol and ketoprofen are small molecule drugs. Propranolol and ketoprofen have similar logP, and M_w (table 1). Therefore the influence of these properties on the release study and iontophoretic study is minimized.

Table 1. A comparison of physicochemical properties between propranolol and ketoprofen (DrugBank, 2013a, 2013b).

	Propranolol	**Ketoprofen**
pKa	9.42	4.45
logP	3.48	3.12
Mw (g/mol)	259.3434	254.2806

10.3. Drug release study

The release test was run in a beaker with a volume of 250 ml. The amount of buffer used was 200 ml. This volume was chosen based on the consideration on the solubility of propranolol and ketoprofen in water. The buffer solution used is a HEPES (25 mM) solution with NaCl (0.9 %). The pH was adjusted to 7.4 with NaOH (2 M). The drug release study was carried out in ambient room temperature.

In the release study, the donor compartment used for containing the loaded gel is a simple septum cap. The mold (septum cap) was attached to the petridish with domestic use super glue (ethyl 2-cyanoacrylate, Loctite Super Glue Brush On brand). The prepared gel was loaded to the septum cap as late as possible prior to the start of each experiment to prevent dehydration of the gel. Mixing was done before each portion of drug loaded gel was fitted into a septum cap with the shape of a cylinder. Only the upper side with an area of a circle was open for drug release from the gel reservoir. The sides and the bottom of the septum cap were solid without openings. The area available for drug release from the septum cap was measured to be 0.49±0.00 cm^2.

In order to prevent the floating of the petridish stand, where the gel filled septum cap is attached, simple weights (3 pcs.) were used. Parafilm was used to cover the opening of the beaker during the release test. This was done to prevent water loss. Each beaker contained a stirbar and a magnetic stirrer was switched on for the whole duration (t = 6 hours) of each test run. The mixing by the magnetic stirrer helps prevent the possibility that the layers of water with higher concentration near the source of release might decrease the diffusion and release of further amounts of drug from the hydrogel source.

In the drug release study, we had three parallels for each set run. One sample was collected at each data collection time point from each parallel beaker. The time points for data collection were at 0, 10, 20, 30, 45, 60, 90, 120, 150, 180, 240, 270, 300, 330 and 360 minutes. All samples were collected and prepared for analysis manually.

10.4. Iontophoretic transdermal permeability study

10.4.1. Porcine skin samples

Porcine ear skin was used as a model for human skin. Raw porcine ears were obtained from pigs most recently slaughtered at a local abattoir. To prevent damaging the skin, these ears had not gone through boiled or high temperature water treatment. After obtaining these ears,

they were gently washed under cold tap water to remove the mud and dirt. Then the excess water was removed with paper towels when necessary while adding 0.9 % NaCl solution in order to prevent drying of the skin tissue. The sample pieces were obtained from the convex side of the ear. The skin was removed from the ears with the help of a scalpel and a pincet. The fat tissue was carefully removed from the skin samples. The hair on the skin was cut short carefully using scissors. The obtained skin samples had full thickness, since no additional procedures, such as tape-stripping, were done. The skin samples were then stored at - 20 °C and thawed overnight before usage. The thawed skin was then temporarily stored in 0.9 % NaCl before the attachment to the actual experimental system.

10.4.2. Iontophoresis setup

The iontophoresis setup was built on Franz diffusion cells. The area available for the drug release from gel through the porcine skin is 2.38 ± 0.10 cm^2. Each glass donor cell and receiver cell were paired to make sure that correct current density passed through reliably.

Pure platinum electrodes and salt bridges were used similarly as previously done by Malinovskaja and coworkers (Malinovskaja et al. 2013). Silicone tubes were filled with KCl (1 M) and gelling was achieved with 2 % agarose powder. A constant current was used (Ministat potentiostat, Sycopel Scientific Ltd., UK). The current was applied for 5 hours and then ceased.

Two different current densities were applied in the iontophoretic study. The higher current density used is 0.5 mA/cm^2 while the lower one was 0.25 mA/cm^2. In addition, passive run was also done in order to obtain a reference for the base line. Both the passive and the iontophoretic runs had a water bath set up at 37 °C for the whole duration of a run (24 hr).

In the iontophoresis study, two parallel samples (100 µl) from each parallel receiver glass cell was taken at each time point. The time points for data collection were at 0, 30, 60, 90,

120, 150, 180, 240, 300 and 1440 minutes. All samples were collected and prepared for analysis manually.

Since the samples from the iontophoresis study contain possibly residues from porcine ear skin, 0.5 % formic acid in acetonitrile (300 µl) was used to treat the samples. The samples were then vortexed briefly (5 s) and then they were put into centrifuge at 15 *g* for 5 minutes. Then 250 µl supernatant was separated and allowed to dry. They were rediluted for UPLC analysis.

10.5. Analysis of the samples

The ultra-performance liquid chromatography (UPLC) system used for the analysis of all collected samples in both studies was Acquity UPLC (Waters, USA).

The UPLC analysis of propranolol samples was done with a UPLC HSS T3 2.1 x 50 mm column (Waters, USA). The column had a particle size of 1.8 µm. The running buffers used were A – 0.015 M KH_2PO_4 (pH 2) and B – 100 % CH_3CN. For propranolol samples, the gradient used was A 80.0 % – B 20.0 % (t = 0), A 40.0 % – B 60.0 % (t = 2.00), A 80.0 % – B 20.0 % (t = 2.01) and A 80.0 % – B 20.0 % (t = 3.00). The retention time was ~1.1 min and the column temperature used was +30 °C. The flow rate was 0.5 ml/min and the injection volume was 5 µl.

The UPLC analysis of ketoprofen samples was done with a UPLC HSS C-18 2.1 x 50 mm column (Waters, USA). The column had a particle size of 1.8 µm. The running buffers used were A – 0.015 M KH_2PO_4 (pH 2) and B – 100 % CH_3CN. For ketoprofen samples, the gradient used was A 70.0 % – B 30.0 % (t = 0), A 30.0 % – B 70.0 % (t = 2.00), A 70.0 % – B 30.0 % (t = 2.01) and A 70.0 % – B 30.0 % (t = 3.00). The retention time was ~1.3 min and the column temperature used was +30 °C. The flow rate was 0.5 ml/min and the injection volume was 5 µl.

10.6. Models and simulations

The models were all built and simulations run using Stella software (version 10.0.3, isee systems). From the experimental release study, a permeability value, P_{app}, under non- perfect sink conditions, was obtained for each drug loaded NFC hydrogel version run, totalling in 18 P_{app} values. The P_{app} values were calculated using equation (1):

$$P_{app} = \frac{dM}{dt} * \frac{1}{(A * C_0)} \qquad \text{equation (1)}$$

where dM/dt is drug released as moles over time, A is the surface area exposed for drug release and C_0 is the initial concentration of the drug loading in NFC hydrogel.

Since there were limited version of the loaded gels tested experimentally, more variations will be tested using simulation models. Based on the solubility of the model drugs propranolol and ketoprofen, a suitable mathematical equation for drug diffusion was selected after the UPLC results were obtained. The equations discussed below are usable if the experimental results verify that cumulative drug release has linear correlation with the squareroot of time.

Equation 2 is for monolithic solutions and equation 3-1 (Higuchi's equation) is for monolithic dispersions (Siepmann and Siepmann 2012). It is obvious that in both cases of a monolithic solution and a monolithic dispersion, the ratio M_t/M_∞ (amount of drug released over amount of drug originally available) is directly proportional to squareroot of time ($\sqrt{t}$).

Equation 4 is a rearranged form of equation 3-1.

$$\frac{M_t}{M_\infty} = 4\sqrt{\frac{Dt}{\pi L^2}} \qquad \text{equation (2)}$$

$$M_t = A\sqrt{DC_s(2C_{\text{ini}} - C_s)t}$$ equation (3-1)

Since C_{ini} (= C_0) is much higher than the solubility of the drug in the reservoir, the term $-C_s$ can be neglected and we have:

$$M_t = A\sqrt{DC_s * 2C_{ini} * t}$$ equation (3-2)

Dividing both sides with M_∞ gives:

$$\frac{M_t}{M_\infty} = \frac{A}{M_\infty}\sqrt{DC_s * 2C_{ini} * t}$$ equation (3-3)

Because $\mathrm{M}_\infty = \mathrm{C}_{\text{ini}} * \mathrm{V}$, then we have:

$$\frac{M_t}{M_\infty} = \frac{A}{\mathrm{C}_{\text{ini}} * \mathrm{V}}\left(\sqrt{DC_s} * \sqrt{2} * \sqrt{C_{ini}} * \sqrt{t}\right)$$ equation (3-4)

Rearranging the above equation gives us:

$$\frac{M_t}{M_\infty} = \frac{A * \sqrt{D\,C_s} * \sqrt{2}}{\mathrm{V} * \sqrt{C_{ini}}} * \sqrt{t}$$ equation (4)

11. Results

It was found that it was not possible to measure the drug loaded NFC hydrogel with a nephelometer (Nepheloskan Ascent 1.5). The solubility in NFC hydrogels for the model drugs, propranolol and ketoprofen, were therefore not determined. The method of analysis

was UPLC for all samples from the release and iontophoresis tests. All results from the experimental part including modelling are presented below.

11.1. pH of NFC hydrogels

The pH of the NFC hydrogels were measured with a pH meter (Table 2 and 3).

Table 2. Measured pH of NFC gels.

Name	% (m/v)	pH (± 0.05)	Temperature (°C)
Gel A (native)	1.65	6.14	21.1
Gel B (anionic)	1.16	6.73	21.1
Gel C (anionic)	1.50	6.61	21.3
Gel D (native)	2.65	6.92	21.7
Gel E (native)	3.27	7.25	23.9
MilliQ water	-	6.02	21.0

Table 3. Average pH of NFC gels.

Gels	average pH	Temperature (°C)
ABCDE	6.73 ± 0.41	21.8 ± 1.2
ABC	6.49 ± 0.31	21.2 ± 0.1
BC	6.67 ± 0.08	21.2 ± 0.1
ADE	6.77 ± 0.57	22.2 ± 1.5

11.2. Results from the release study

From these release tests, we obtained experimental values for M_t and M_∞, which stand for absolute cumulative amounts of drug released from the loaded gels at different time points and are described in detail elsewhere (Siepmann and Peppas 2001).

The results presented in table 4 are expressed as wt. % released at 6 hours, calculated based on the ratio M_t/M_∞, where M_∞ is equal to the initial amount of drug available for release in the NFC hydrogel.

Table 4. Release tests: percentages released from initial loading at t = 6 hours.

	wt.% released					
Loading (mg/g)	PinA	PinB	PinC	KinA	KinB	KinC
10	80.9 ± 2.4	79.6 ± 5.0	100.1 ± 9.8	86.3 ± 8.9	80.5 ± 4.6	84.6 ± 2.8
30	88.8 ± 1.3	86.6 ± 6.2	92.5 ± 3.4	55.9 ± 3.7	51.6 ± 2.4	58.4 ± 3.1
90	81.1 ± 5.7	78.3 ± 4.3	75.0 ± 8.0	32.6 ± 1.9	30.4 ± 1.3	31.9 ± 2.5

The whole release profiles produced by the different initial loading concentrations of drug in each NFC hydrogel are displayed in graphs 1 and 2. Next, it was compared, if the initial loading concentrations caused a different release profile when a different type of NFC hydrogel was used (graphs 3 and 4).

In addition, it was checked if the amount of drug released had a linear correlation with the squareroot of time, in order to determine the suitable mathematical equations, which can be used for simulations models (graphs 5 and 6). The general trend for mass percentages released over squareroot of time for both drugs are shown in graphs 7 and 8.

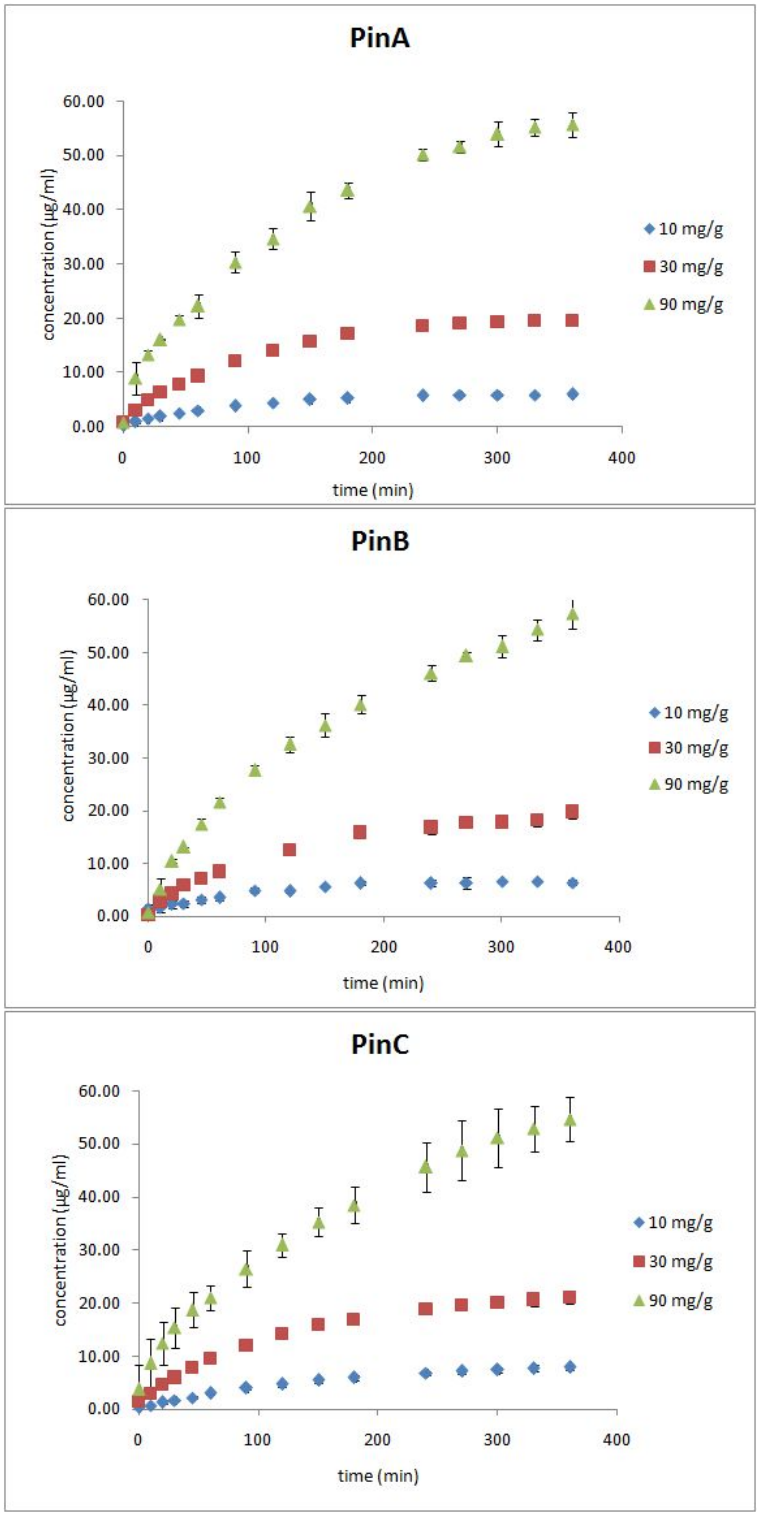

Graph 1. The concentration of released propranolol over time in minutes. For each gel (A, B and C) three different drug concentrations (10 mg/g, 30 mg/g, 90 mg/g) were loaded.

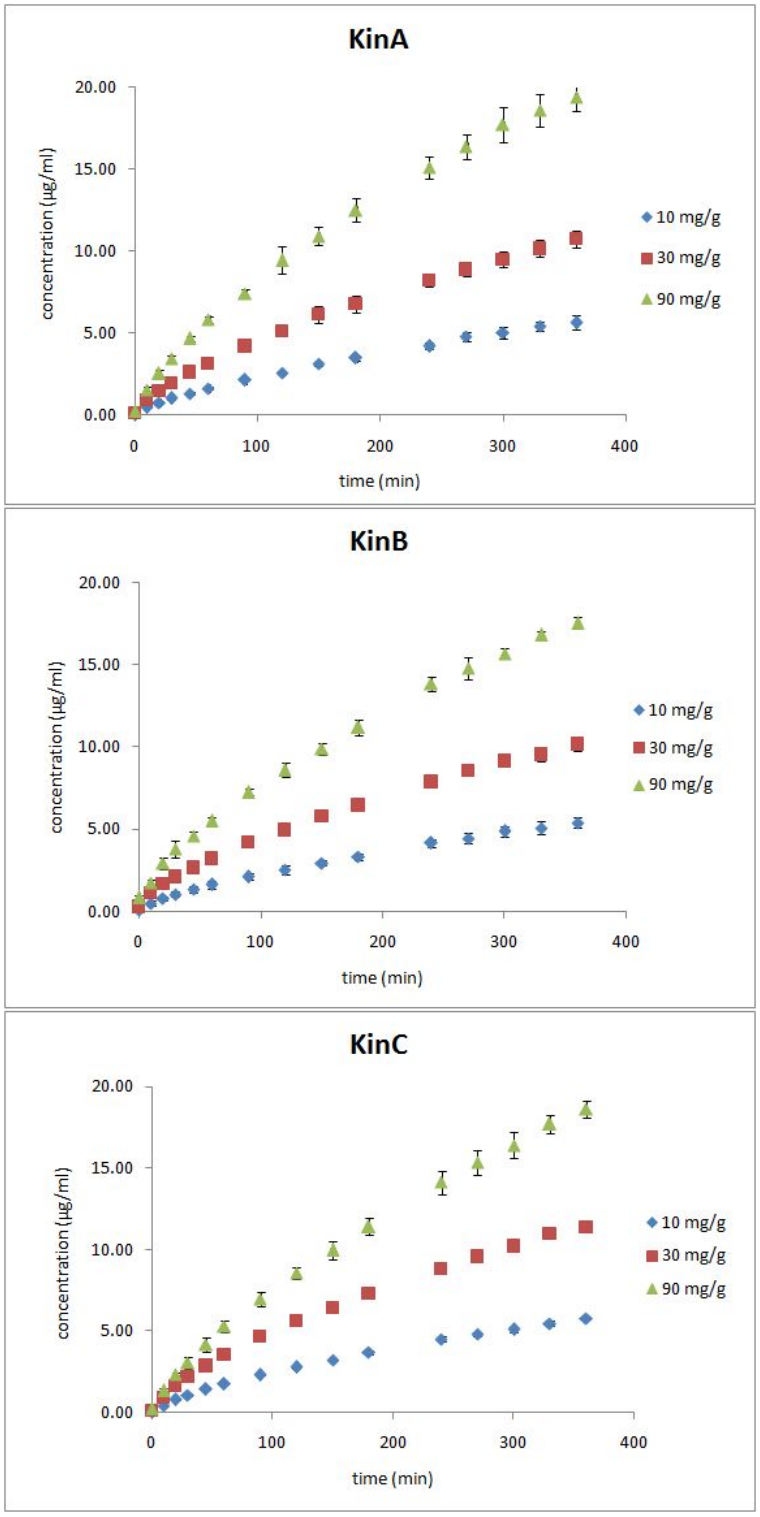

Graph 2. The concentration of released ketoprofen over time in minutes. For each gel (A, B and C) three different drug concentrations (10 mg/g, 30 mg/g, 90 mg/g) were loaded.

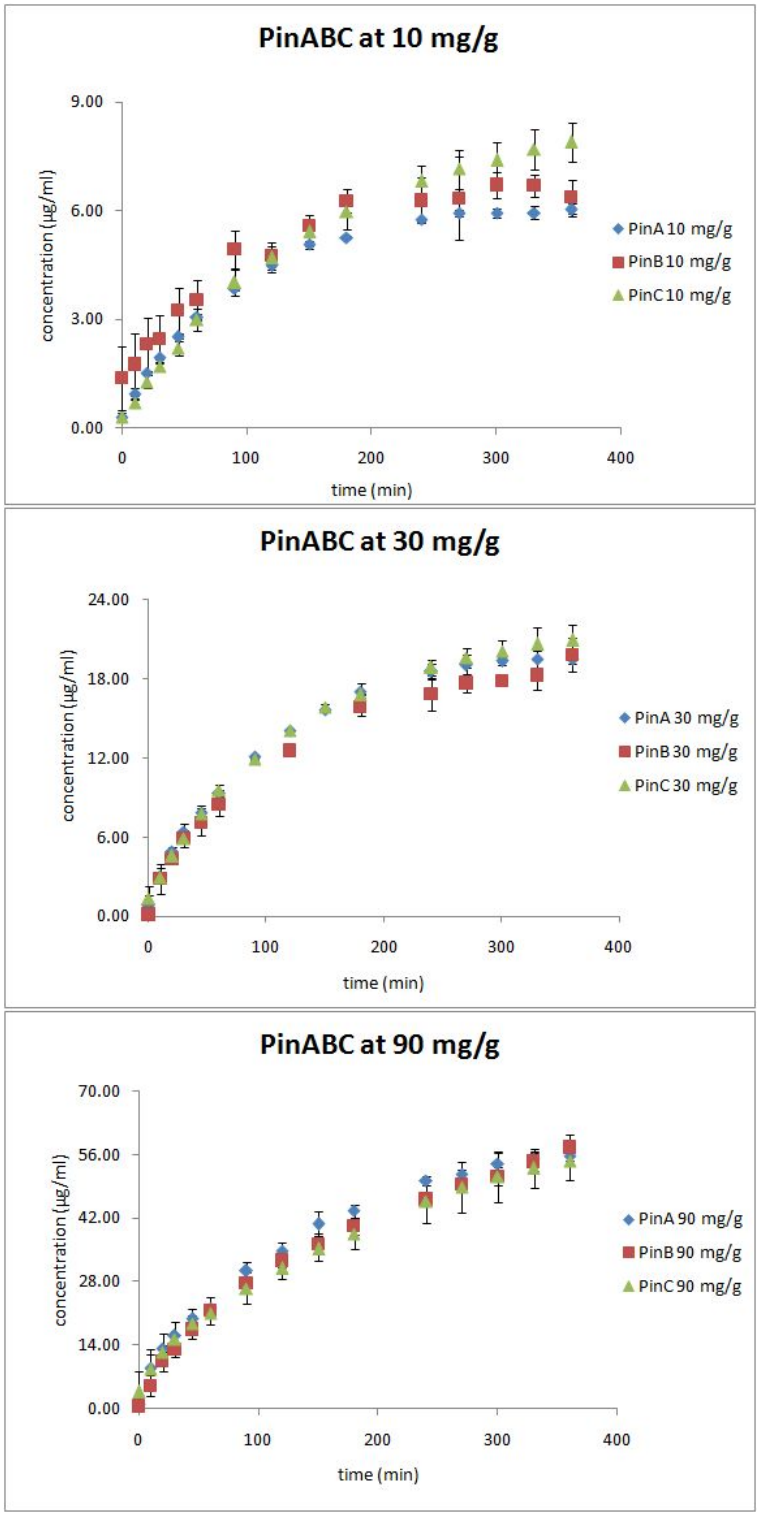

Graph 3. Released propranolol concentration from different NFC hydrogels are similar to each other when the loaded drug concentration remains unchanged.

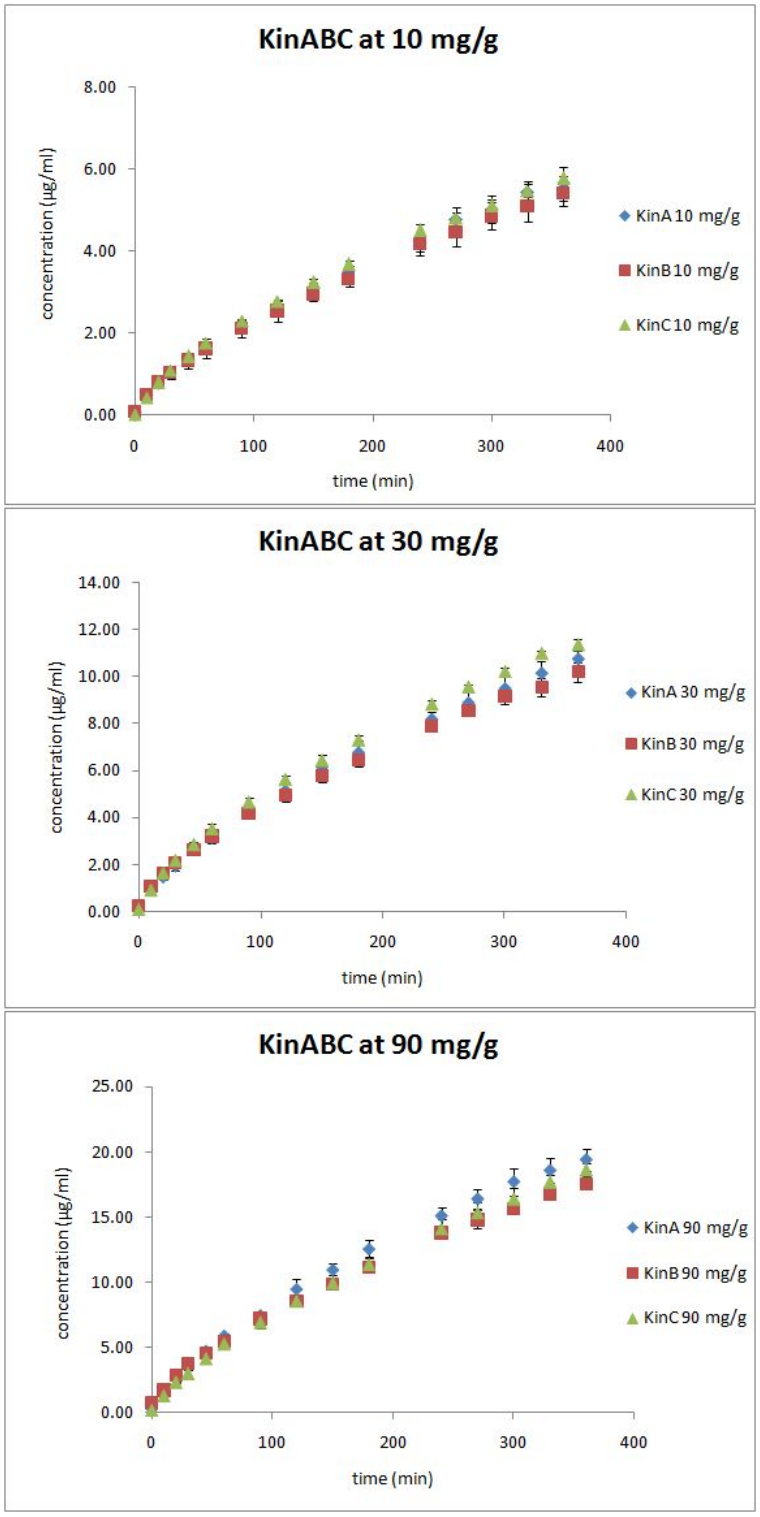

Graph 4. Released ketoprofen concentration from different NFC hydrogels are similar to each other when the loaded drug concentration remains unchanged.

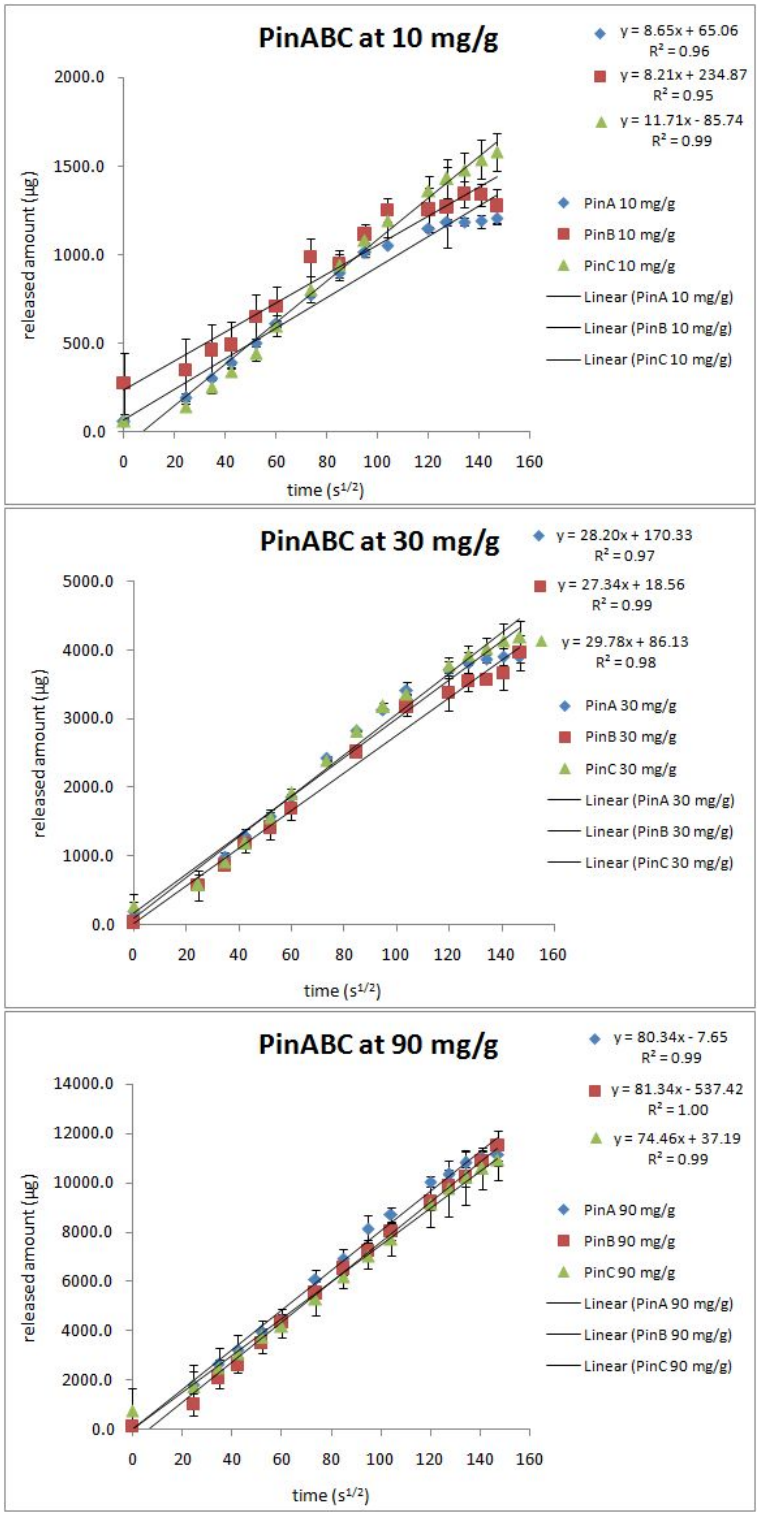

Graph 5. Loading concentration affects the amount of propranolol released for all NFC hydrogels used. The released amount has a linear correlation with time expressed in squareroot of seconds.

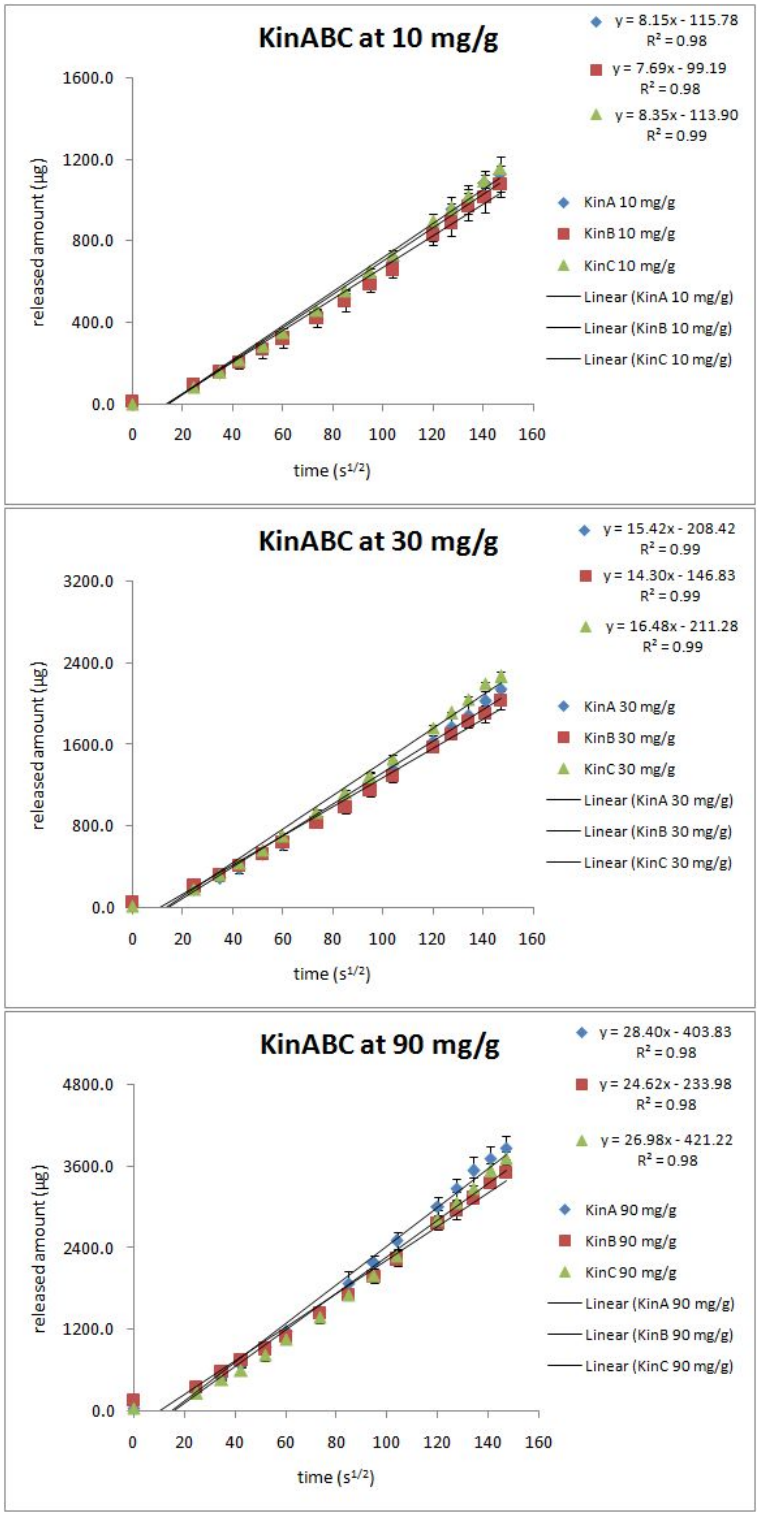

Graph 6. Loading concentration affects the amount of ketoprofen released for all NFC hydrogels used. The released amount has a linear correlation with time expressed in squareroot of seconds.

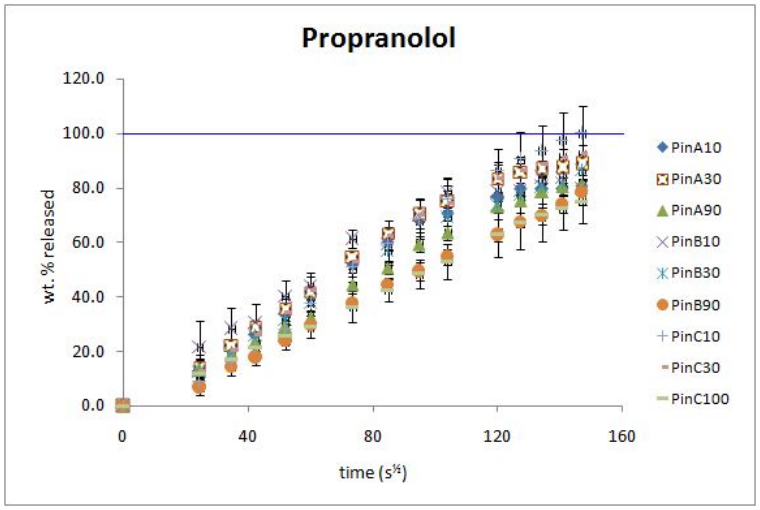

Graph 7. Propranolol released from gel A, B and C over squareroot of time in seconds. A line is marked at 100 % released.

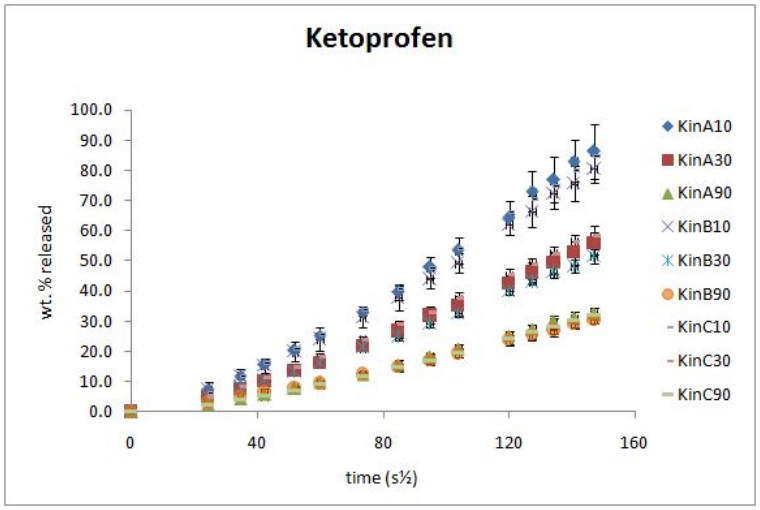

Graph 8. Ketoprofen released from gel A, B and C over squareroot of time in seconds.

Table 5. Release of propranolol until 60 % freed.

	Propranolol wt. % released								
time (min)	PinA10	PinA30	PinA90	PinB10	PinB30	PinB90	PinC10	PinC30	PinC90
60				44.0±4.8					
90	51.8±1.6	54.4±1.6		61.4±3.4				52.9±4.1	
120	60.2±2.9	63.3±2.3		59.3±2.5	56.8±0.0		59.6±6.2	62.4±5.5	
150			59.2±2.9	69.7±5.8	-		68.7±7.6		
180			63.5±2.5		69.4±5.1	54.7±2.8			52.9±6.3
240						62.7±2.5			62.8±8.4

Table 6. Release of ketopforen until 60 % freed.

	Ketoprofen wt. % released								
time (min)	KinA10	KinA30	KinA90	KinB10	KinB30	KinB90	KinC10	KinC30	KinC90
90									
120									
150									
180	53.5±4.3			49.4±3.2			54.0±2.1		
240	64.3±5.8			61.9±3.5			66.0±2.3		
270									
300									
330									
360		55.9±3.7	32.6±1.9		51.6±2.4	30.4±1.3		58.4±3.1	31.9±2.5

From table 5 and 6, we see that the time, at which 60 wt. % is released from reservoir, is much more consistent with ketoprofen (10 mg/g, in gels A, B and C) than propranolol. For propranolol, a higher percentage is released in a shorter amount of time. In addition, drug loading does not seem to affect the release of propranolol, whereas for ketoprofen, drug loading is a decisive factor influencing the release percentage over the same time period.

11.3. Results from the iontophoresis study

Table 7. Iontophoresis on skin. Percentages that permeated through within 24 hours.

	wt. % released					
	passive		iontophoretic low		iontophoretic high	
gel type	at 5 hr	at 24 hr	at 5 hr	at 24 hr	at 5 hr	at 24 hr
PinA30	0.02±0.01	0.49±0.06	0.75±0.09	7.33±1.49	0.68±0.29	6.33±3.08

Table 7 shows the effect of both iontophoretic sets and passive reference. The passive flux is included in the iontophoretic values. The drug permeation was enhanced through applied current for a duration of 5 hours. For the iontophoresis study, 3 parallels were used for each version run. A lag time before the drug permeation starts to take place can be observed (graph 9). More drug permeates the skin within 24 hours, when current is applied compared to the passive version (graph 10).

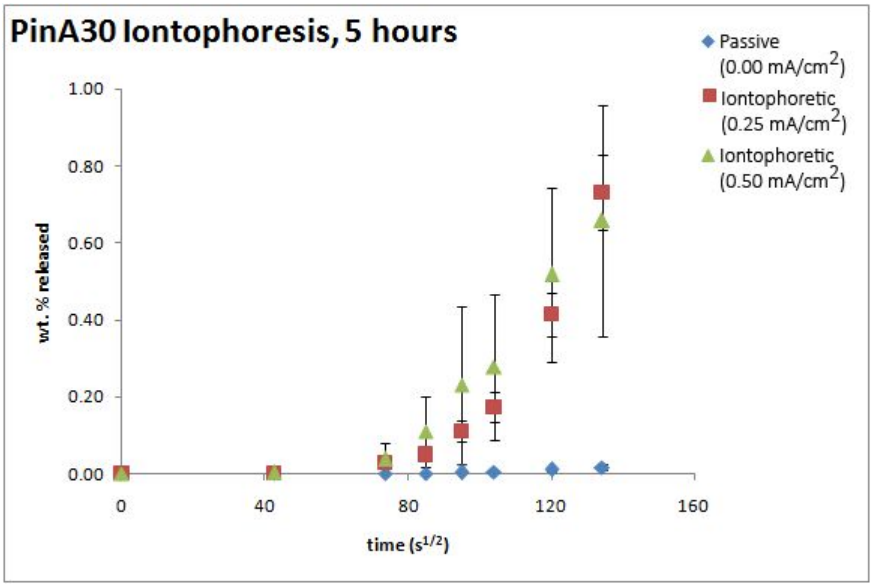

Graph 9. Average cumulative wt. % propranolol released in iontophoretic tests. The drug loading is 30 mg/g. The time is expressed in squareroot of seconds. The last time point displayd in the graph was collected at 5 hours.

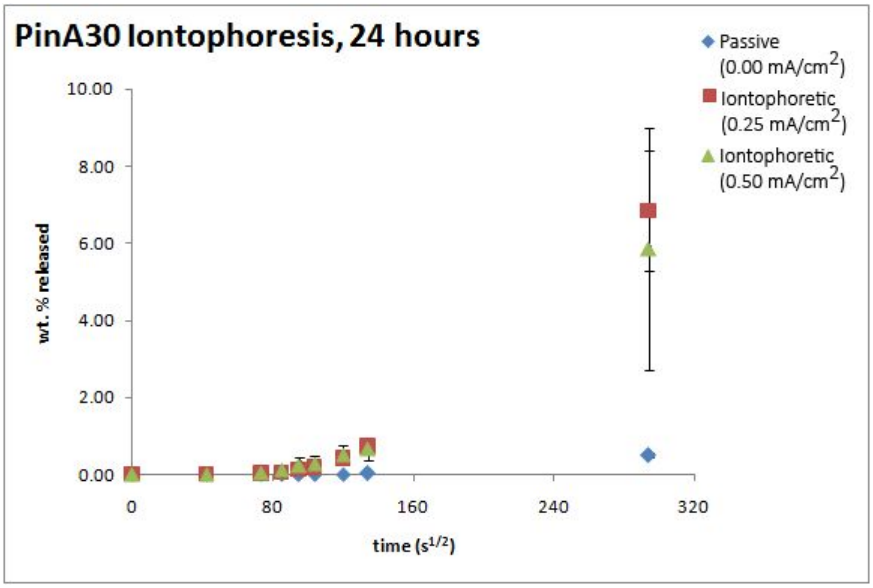

Graph 10. Average cumulative wt. % propranolol released in iontophoretic tests. The drug loading is 30 mg/g. The time is expressed in squareroot of seconds. The last time point displayd in the graph was collected at 24 hours.

The peak value of enhancement drug permeation through porcine skin is 4670 % at 0.25 mA/cm^2. The peak value is 14200 % at 0.50 mA/cm^2. The results displayed in graph 11 were compared with ANOVA analysis (see further details in Appendix A). The p-value obtained was 0.94. This indicates that using the higher current density did not bring a significant added value that the lower current density did not already achieve for drug release.

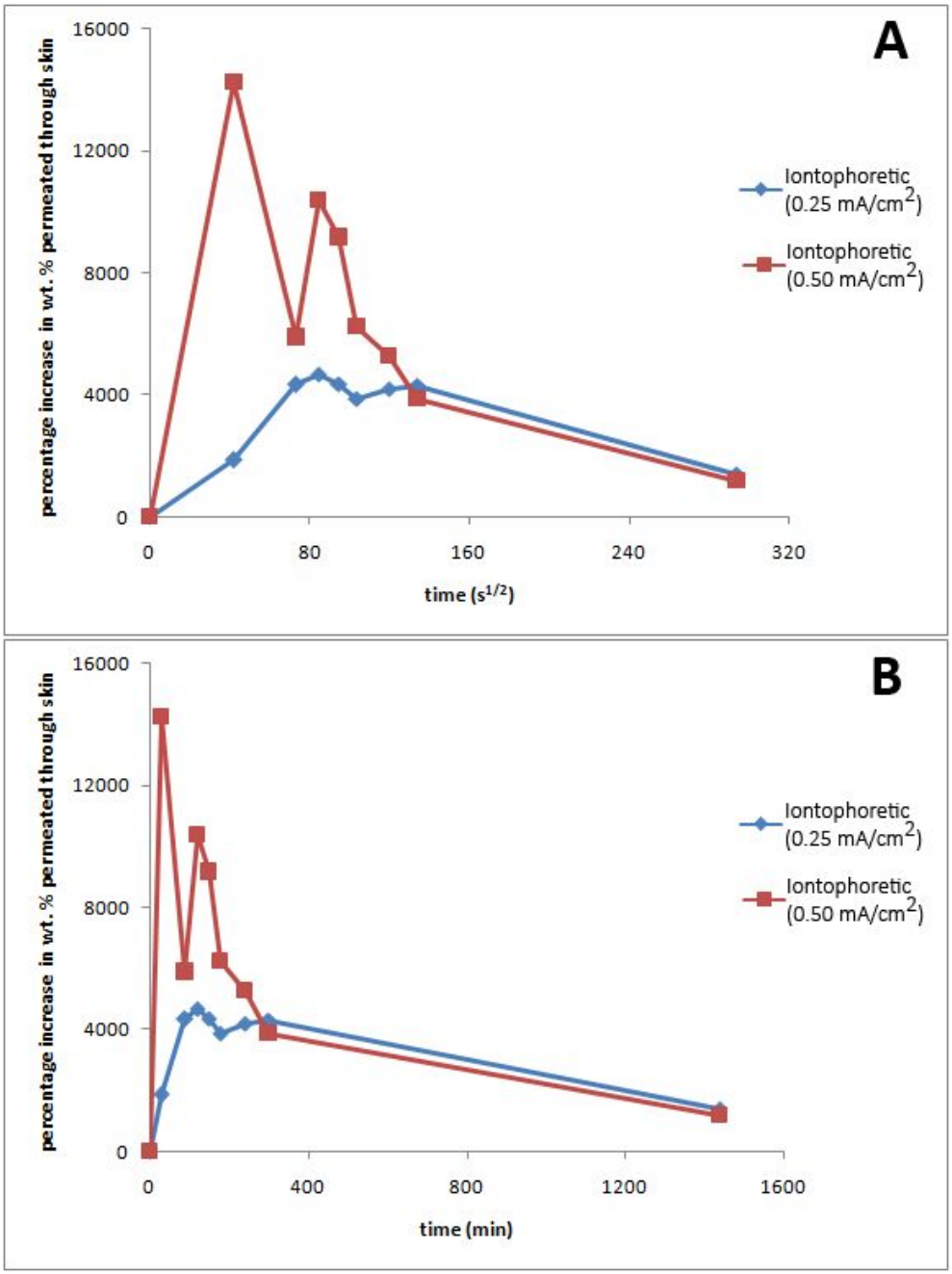

Graph 11. The percentage increase in wt. % that permeated through the porcine skin compared to passive release data during and after iontophoresis. A) The time is expressed in squareroot of seconds. B) The time is expressed in minutes. The last time point displayed in the 5A an 5B was collected at 24 hours.

11.4. Permeability

The apparent permeability (P_{app}) were determined for both propranolol and ketoprofen based on the results obtained from the release study. In addition, based on the data from the iontophoresis study, additional P_{app} values for propranolol was calculated. They are presented in tables 8, 9 and 10. All the P_{app} values were calculated using equation 1. The approaching plateau phase of the release was not taken into account.

Table 8. P_{app} values for propranolol based on data from the release study.

	P_{app} (cm/s)				
NFC Hydrogel	**10 mg/g**	**30 mg/g**	**90 mg/g**	**Average**	**SD**
Propranolol in gel A	2.50E-05	2.07E-05	1.40E-05	1.99E-05	5.55E-06
Propranolol in gel B	1.53E-05	1.52E-05	1.48E-05	1.51E-05	2.57E-07
Propranolol in gel C	2.48E-05	2.16E-05	1.21E-05	1.95E-05	6.63E-06
Average	2.17E-05	1.92E-05	1.36E-05		
SD	5.52E-06	3.49E-06	1.41E-06		

Table 9. P_{app} values for ketoprofen based on data from the release study.

	P_{app} (cm/s)				
NFC Hydrogel	**10 mg/g**	**30 mg/g**	**90 mg/g**	**Average**	**SD**
Ketoprofen in gel A	1.21E-05	8.25E-06	4.46E-06	8.28E-06	3.84E-06
Ketoprofen in gel B	1.09E-05	7.37E-06	3.84E-06	7.37E-06	3.53E-06
Ketoprofen in gel C	1.22E-05	8.30E-06	4.28E-06	8.26E-06	3.96E-06
Average	1.17E-05	7.97E-06	4.19E-06		
SD	7.28E-07	5.25E-07	3.19E-07		

Table 10. P_{app} values for propranolol based on data from the iontophoresis study.

	Papp (cm/s)		
Gel	**passive**	**0.25 (mA/cm²)**	**0.50 (mA/cm²)**
Propranolol in gel A (30 mg/g)	4.40E-08	2.61E-07	1.59E-07

In addition, D for propranolol was determined based on equation (1),

$$\frac{M_t}{M_\infty} = 4\left(\frac{Dt}{\pi L^2}\right)^{1/2} \quad (1)$$

The average diffusion coefficient of propranolol based on 30 mg/g loading in gels A, B and C is $3.65*10^{-3} \pm 0.37*10^{-3}$ cm^2/hr. This value of D is applicable within the limit set by equation (1), which is when $\frac{M_t}{M_\infty} \leq 0.6$ (Siepmann and Siepmann 2012).

11.5. Experimental density of NFC hydrogels

Due to the proprietary nature of the NFC hydrogels used in the experimental part, there were no details on the density of the hydrogels available. An experimental density of 0.90 kg/l was obtained for the drug loaded NFC hydrogels based on 54 measurements when weighing the loaded gels for the drug release study. The experimental density will also be used in the simulation models in the next section.

11.6. Modelling

Based on the experimental results obtained, as presented in the previous section, models were built to further understand the release behaviour of the drug from the NFC hydrogels.

11.6.1. Models based on the release study

In order to choose the proper mathematical model for drug release, the properties of the prepared controlled release system need to be understood (Siepmann and Siepmann 2012). The ketoprofen loaded gels were monolithic dispersions. The propranolol loaded gels were monolithic solutions. The chosen mathematical equations are applicable to diffusion controlled drug release.

The obtained experimental results verified that for both drugs, the amount of drug released has a strong linear correlation ($R^2 \geq 0.95$) with the squareroot of time in seconds (graph 5 and 6). Therefore, the mathematical equations containing term $\sqrt{t}$ for the squareroot of time can be used in the simulation models.

Two types of simulation models were built based on results from the release study.
One model (figure 5) used equation 2 and it was used for propranolol release from NFC hydrogel simulations. Similarly, a model for ketoprofen release was built using equation 3-3 (figure 6). For details regarding the structure of the models, please see Appendix B.

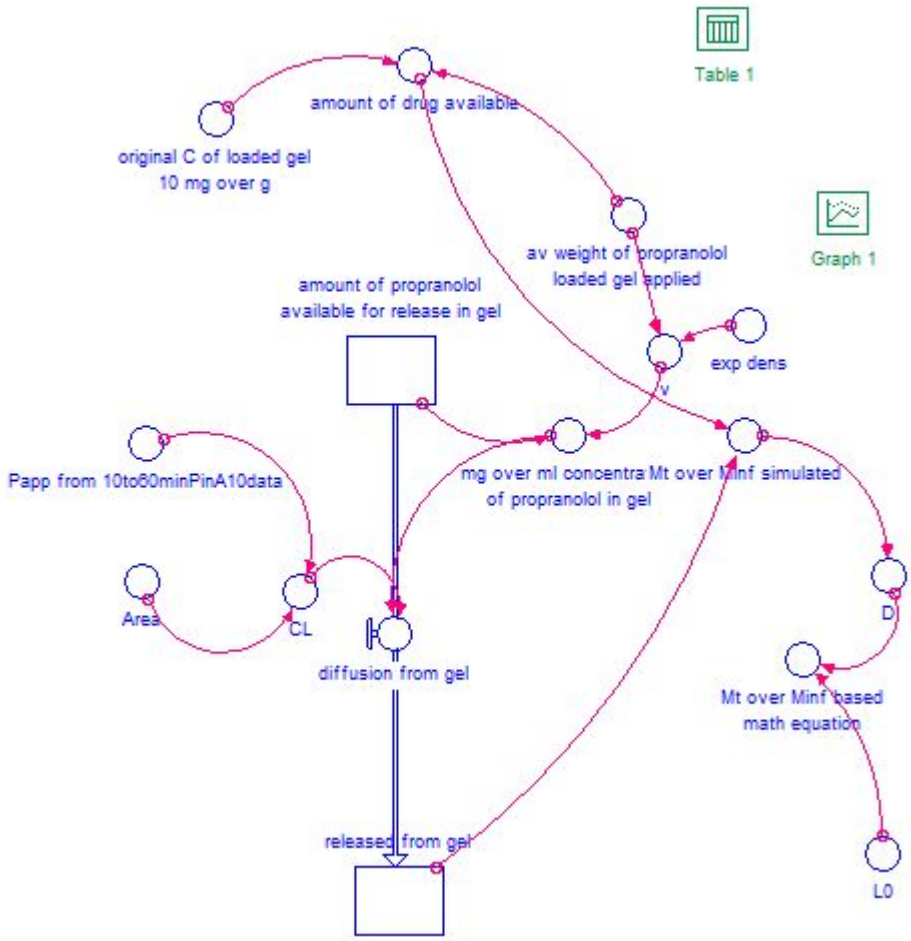

Figure 5. Stella simulation model for propranolol release from NFC hydrogels A, B and C.

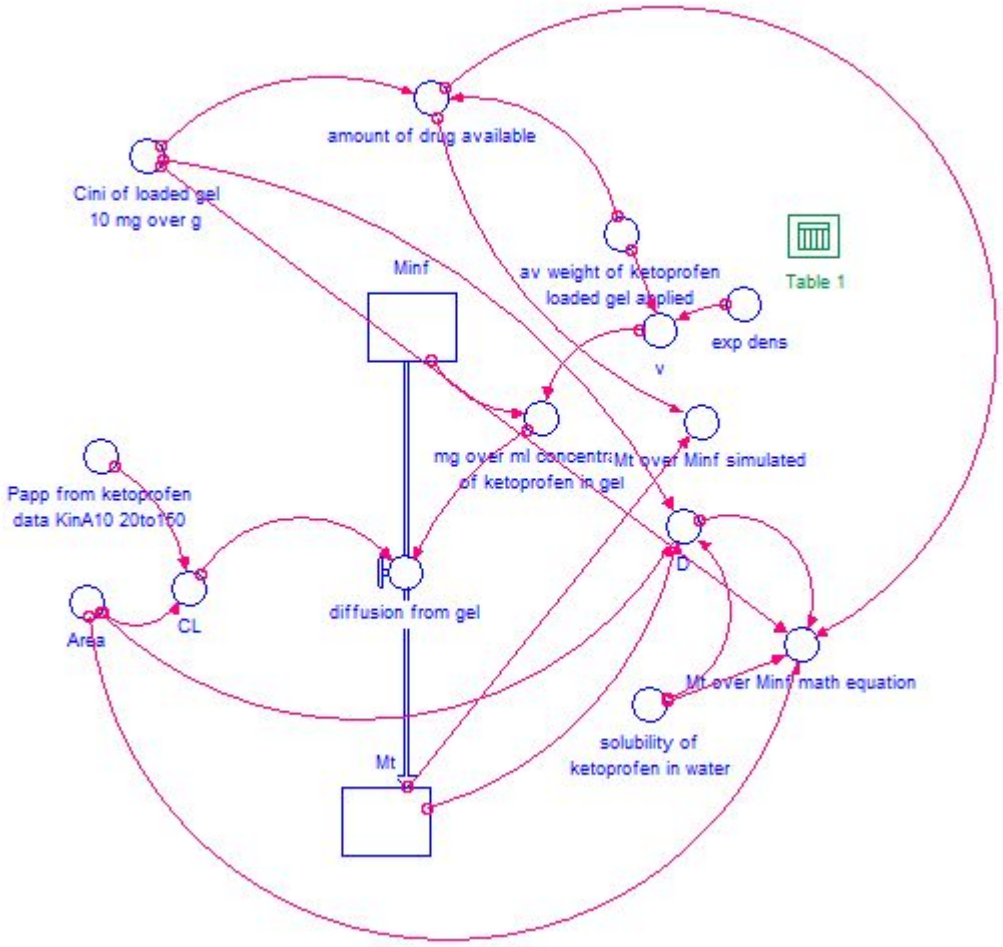

Figure 6. Stella simulation model for ketoprofen release from NFC hydrogels A, B and C.

11.6.2. Simulations based on the release study

The results from the simulations based on the release study are presented below.

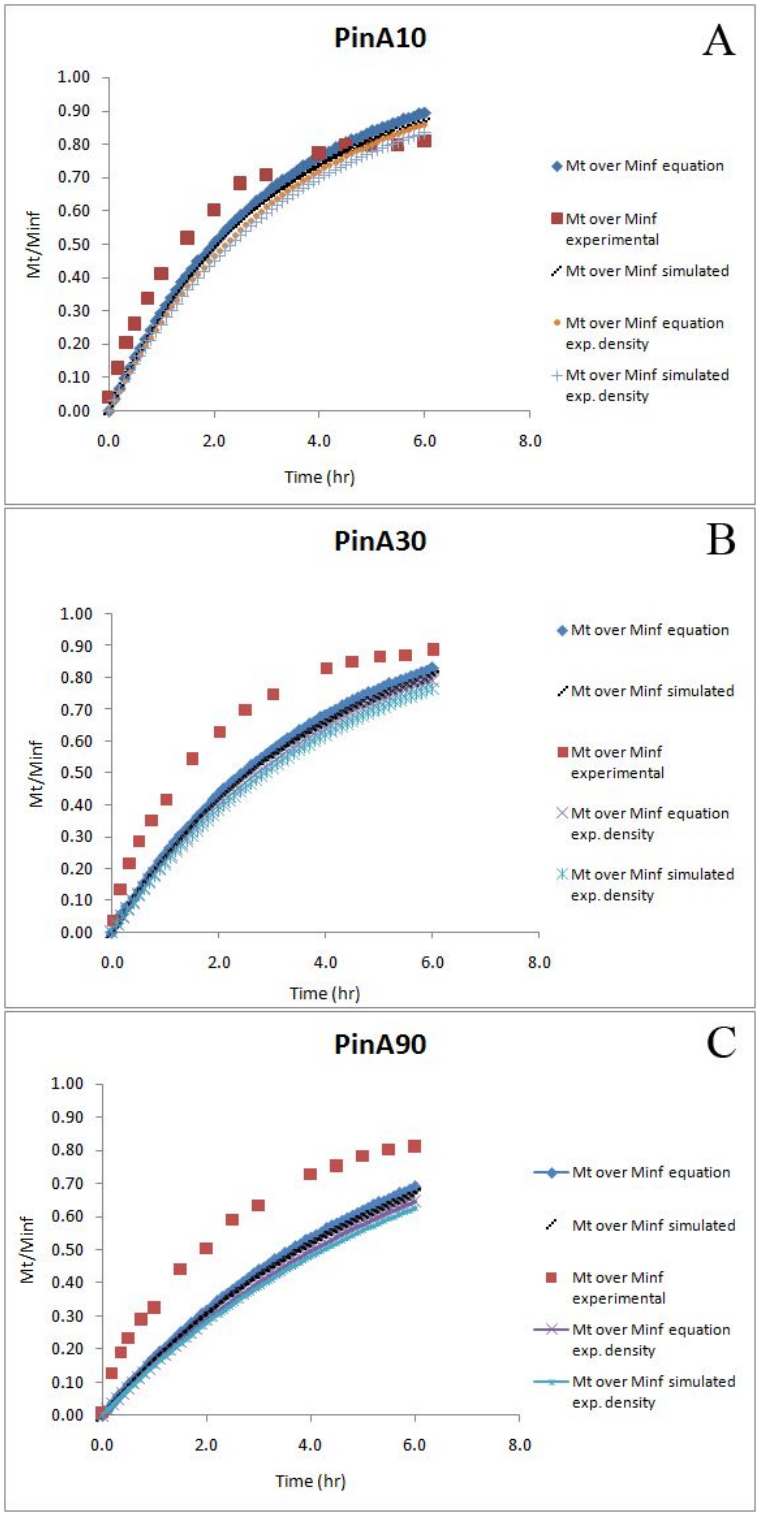

Graph 12. Release simulation for propranolol from hydrogel A with initial loading concentrations at 10 mg/g (A), 30 mg/g (B) and 90 mg/g (C).

Graph 12 shows both experimental (red squares) and simulated release of propranolol from hydrogel A at three different initial loading concentrations. In the model, both the simulation based on experimental data and the mathematical simulation based on equation 2 give similar results. In addition, using the experimental density (0.9 kg/l) or the assumed density (1.0 kg/l) for the NFC hydrogels did not appear to have a prominent effect on the simulated release profile.

Graphs 13 and 14 show the simulations results for propranolol in hydrogels B and C, which are both anionic hydrogels. For these simulations, the experimental density was also applied.

Graphs 15, 16 and 17 show the simulation results for ketoprofen in hydrogels A, B and C. The same experimental density was applied in these simulations as well.

Graph 18 shows how variations in different parameters affect the ratio of drug released from the NFC hydrogel. Using sensispec option, area exposed for release (Graph 18A), length of mold (Graph 18B) and P_{app} value (Graph 18C) were varied.

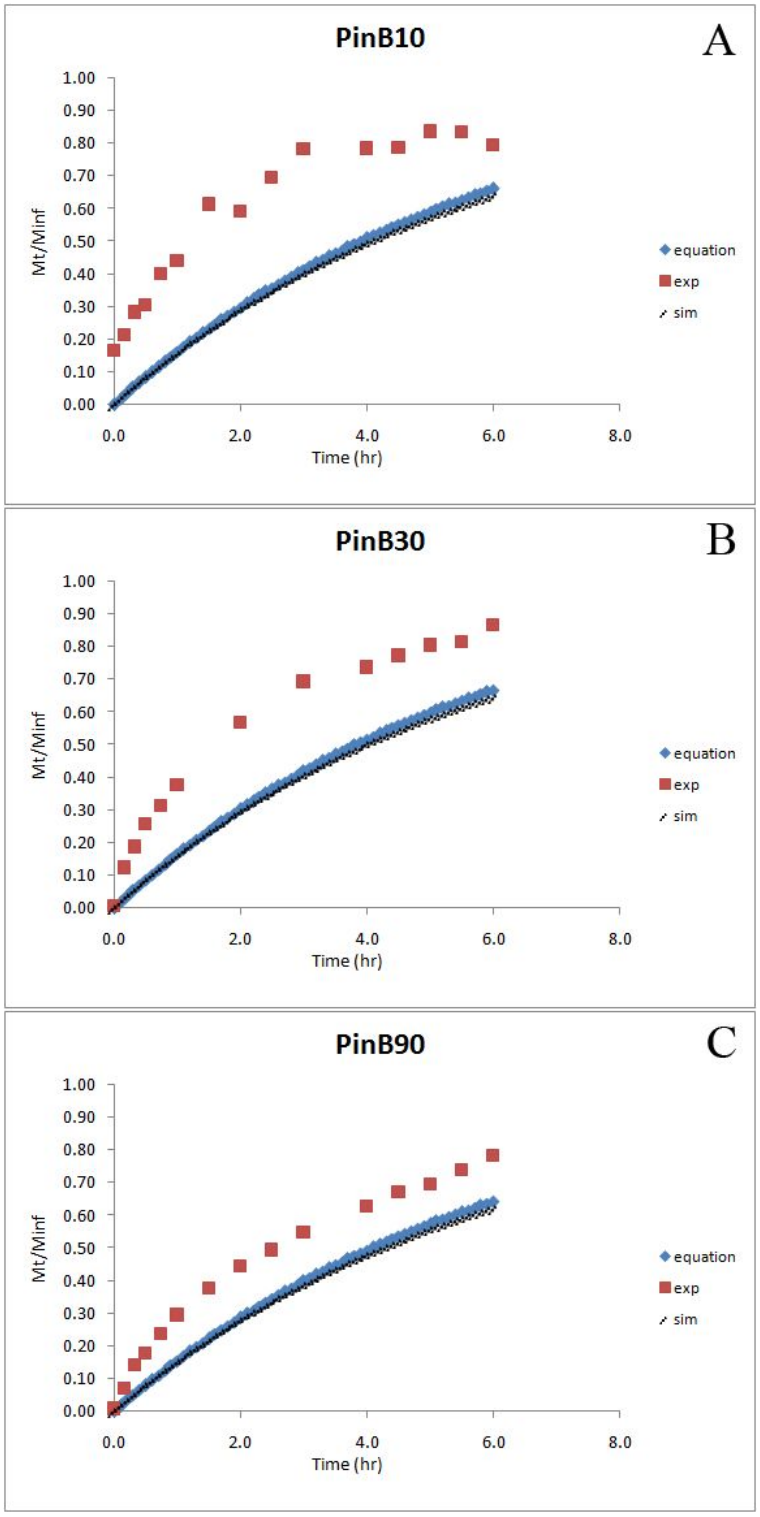

Graph 13. Release simulation for propranolol from hydrogel B with initial loading concentrations at 10 mg/g (A), 30 mg/g (B) and 90 mg/g (C).

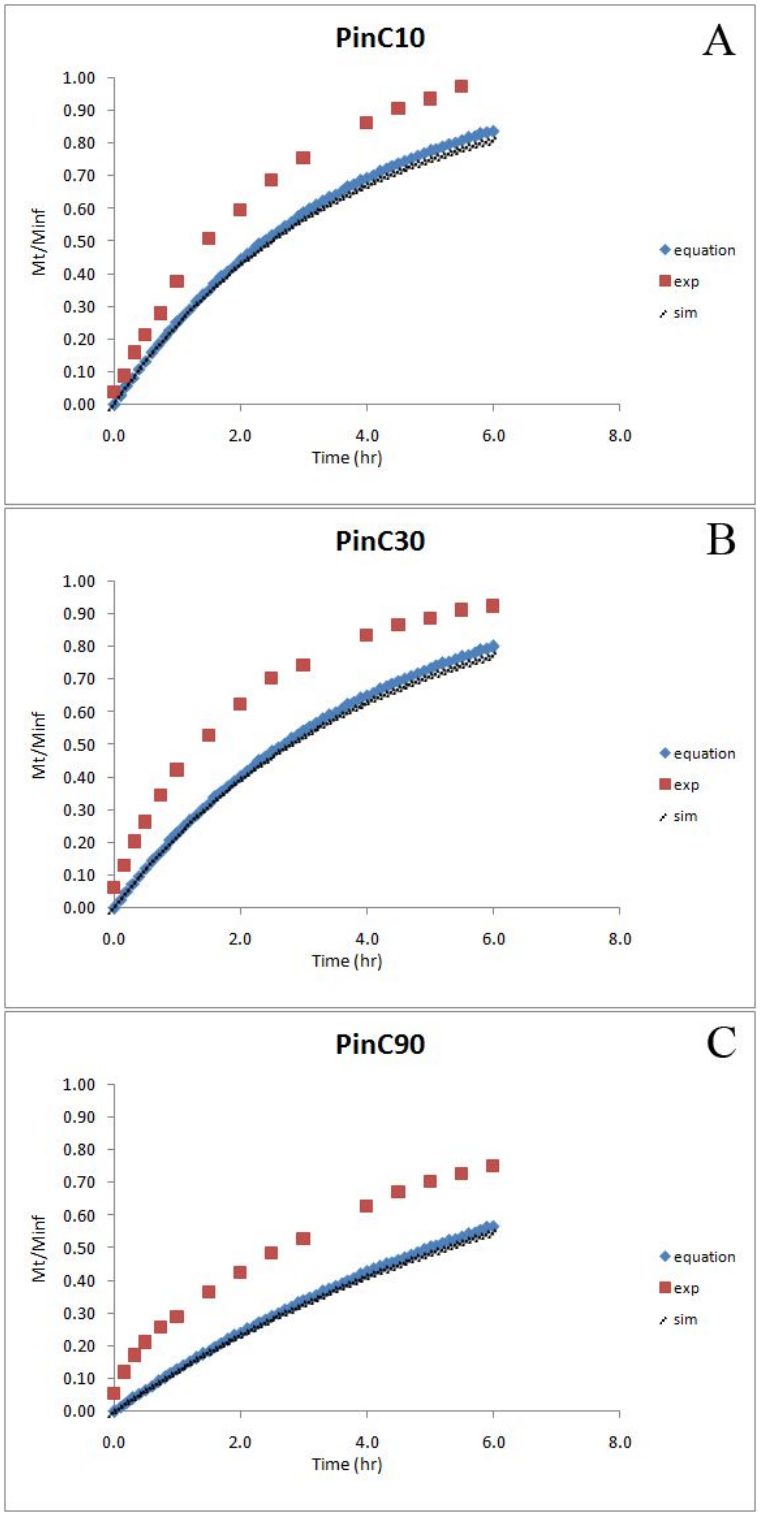

Graph 14. Release simulation for propranolol from hydrogel C with initial loading concentrations at 10 mg/g (A), 30 mg/g (B) and 90 mg/g (C).

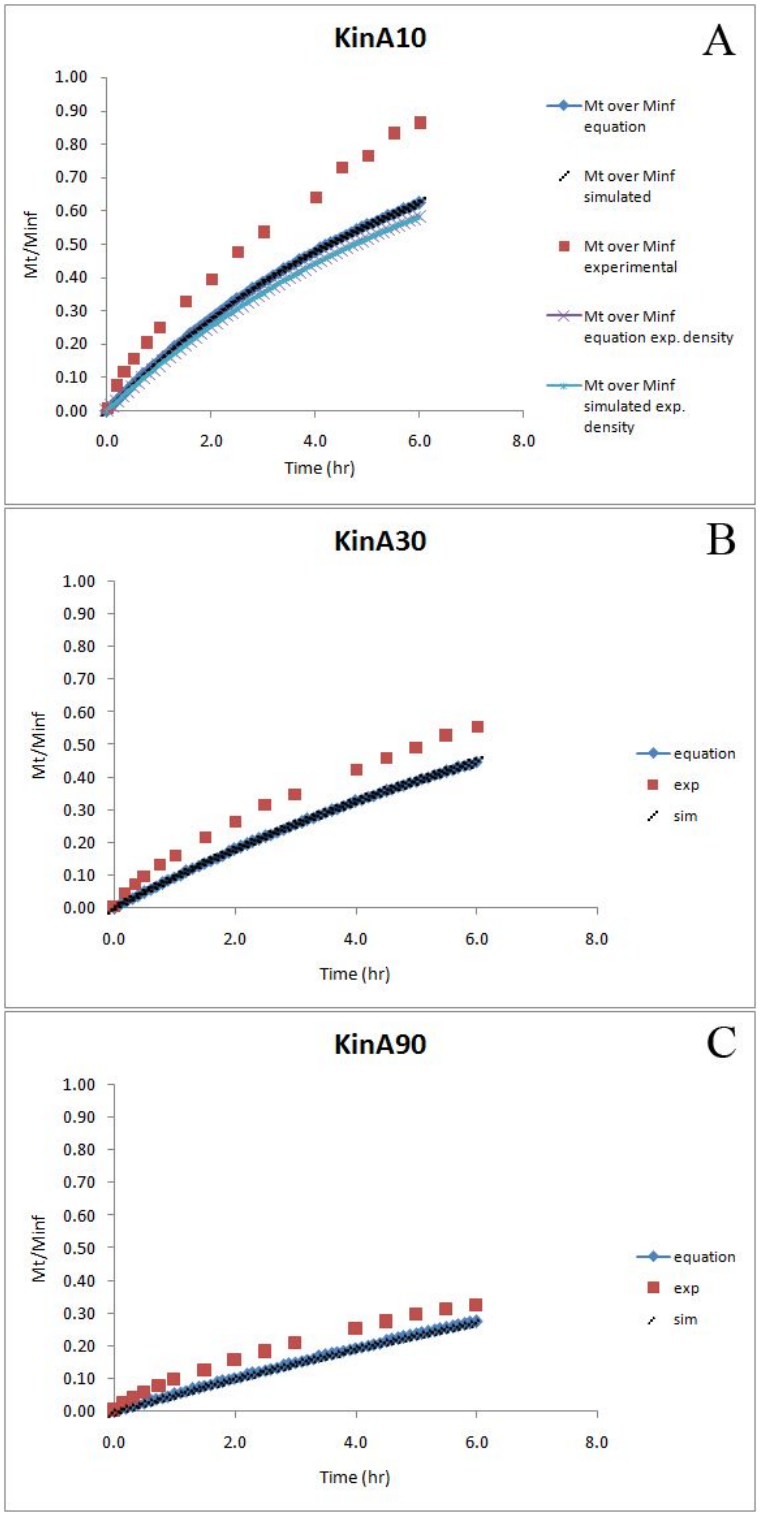

Graph 15. Release simulation for ketoprofen from hydrogel A with initial loading concentrations at 10 mg/g (A), 30 mg/g (B) and 90 mg/g (C).

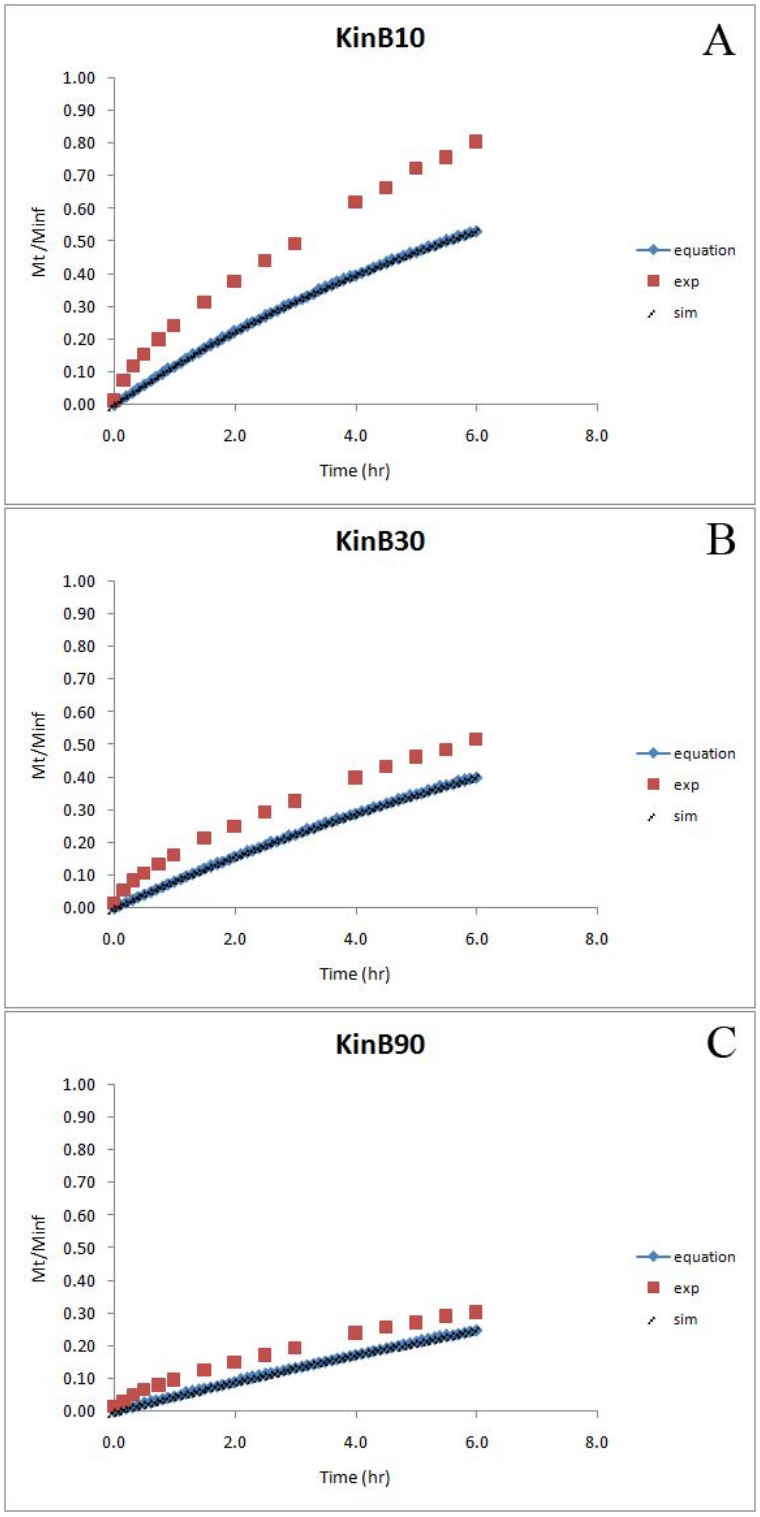

Graph 16. Release simulation for ketoprofen from hydrogel B with initial loading concentrations at 10 mg/g (A), 30 mg/g (B) and 90 mg/g (C).

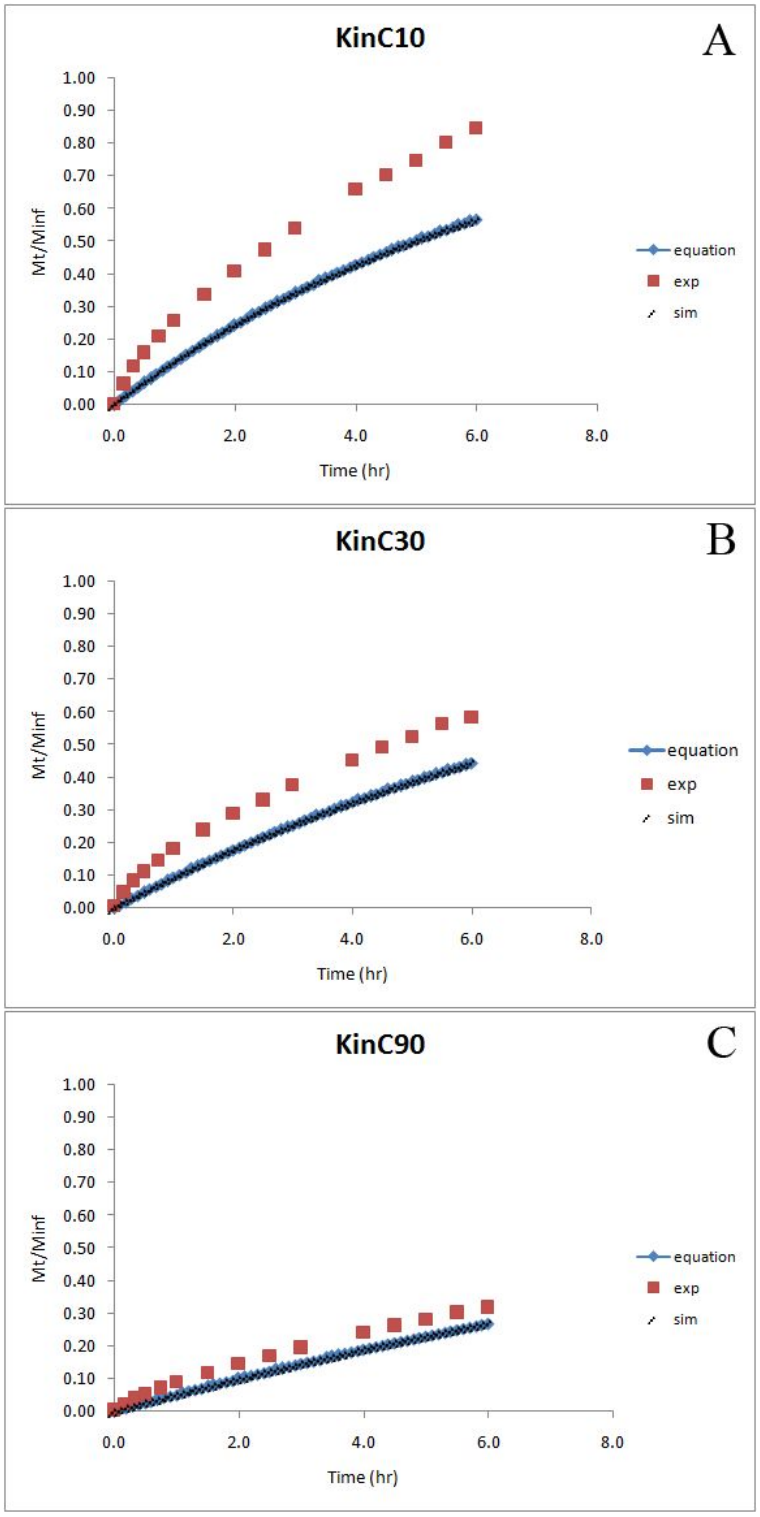

Graph 17. Release simulation for ketoprofen from hydrogel C with initial loading concentrations at 10 mg/g (A), 30 mg/g (B) and 90 mg/g (C).

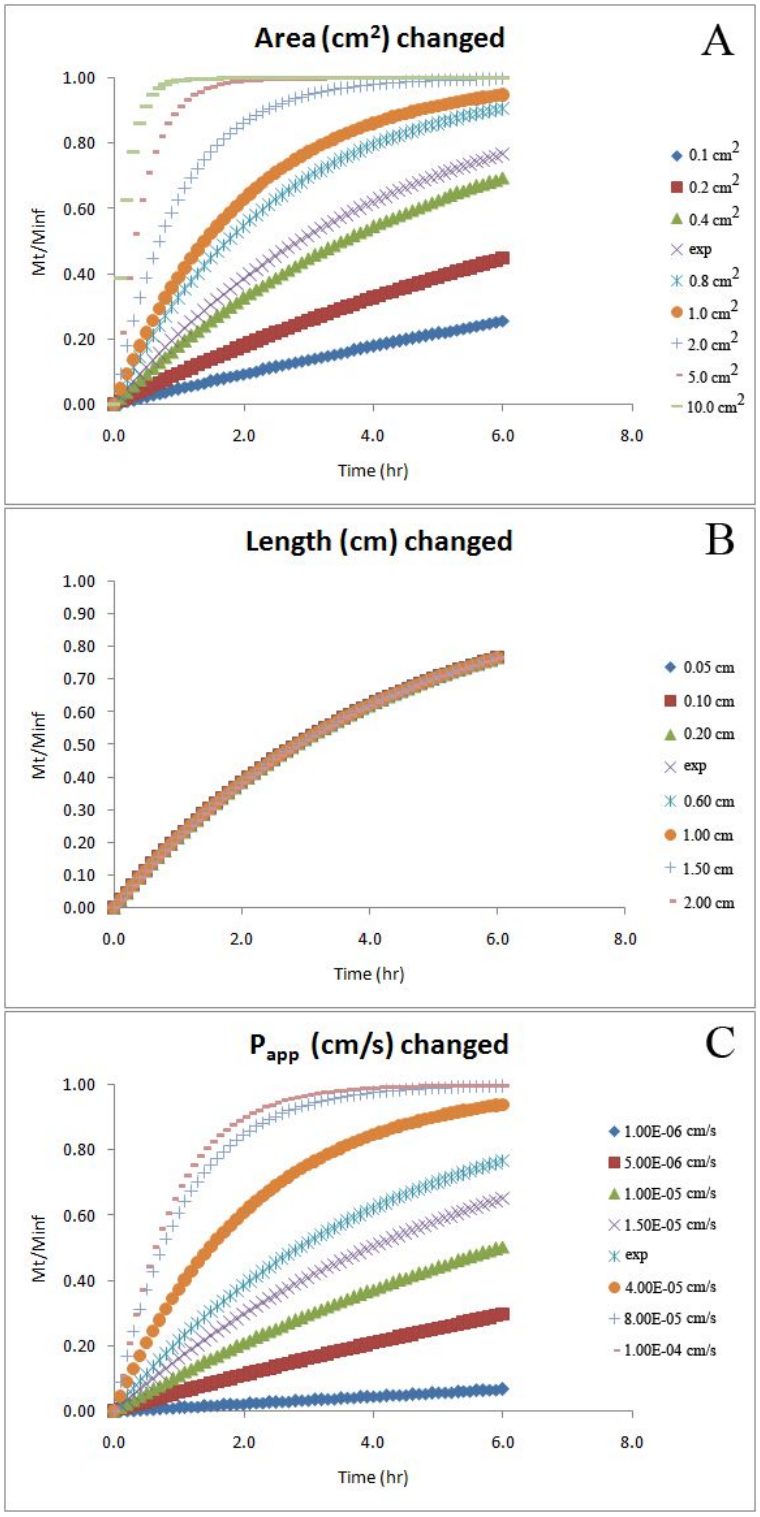

Graph 18. Release simulation for propranolol from hydrogel A with an initial loading concentration at 30 mg/g, when area (cm^2) exposed for release (A), length (cm) of mold (B) and P_{app} (cm/s) (C) is varied.

11.6.3. Model based on the iontophoresis study

A model was built based on the experimental values obtained from the iontophoresis study (figure 7). No mathematical equations were applied for this model.

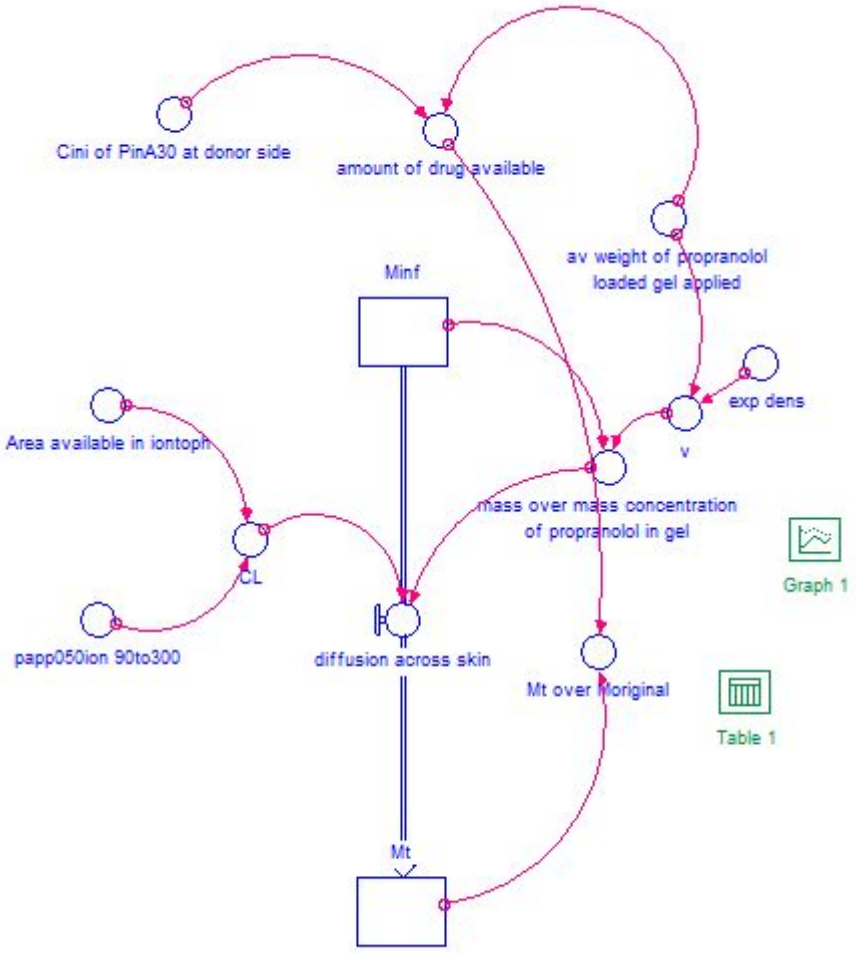

Figure 7. Stella simulation model for propranolol release from NFC hydrogel A under iontophoresis.

11.6.4. Simulations based on the iontophoresis study

Below in Graph 19, the simulations based on the model (figure 7) are shown.

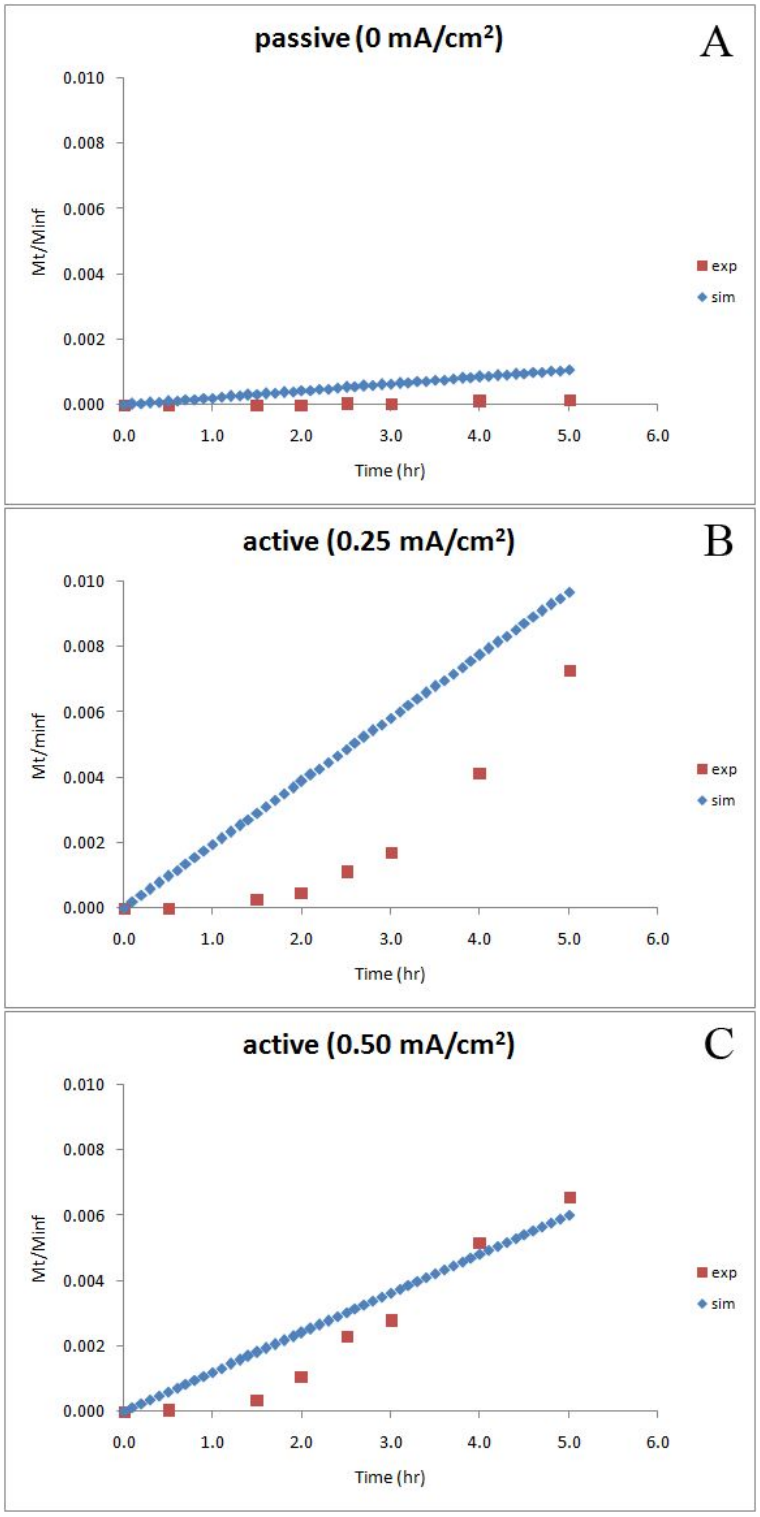

Graph 19. Release simulation for propranolol from hydrogel A with an initial loading concentration at 30 mg/g under different current densities: 0 mA/cm^2 (A), 0.25 mA/cm^2 (B) and 0.50 mA/cm^2 (C).

12. Discussion

12.1. Release study

The results from the release tests (table 4) indicate that for propranolol the degree of drug loading has little effect on the cumulative weight percentage of drug released from the gel. In contrast, for ketoprofen a higher drug loading resulted in a smaller cumulative weight percentage of drug released, indicating that the limit to the rate of release for ketoprofen from the gel is reached more quickly than in case of propranolol. The wt. % released from propranolol loaded NFC hydrogels is higher than in ketoprofen loaded ones for higher initial loading concentrations at 30 mg/g and 90 mg/g.

It should be highlighted that the solubility of the propranolol is between 33.3 g/l and 100 g/l while the solubility of ketoprofen is less than 0.1 g/l (European Pharmacopoeia 2013). Therefore, since all NFC hydrogels used contained a very high water content of over 98 %, the insolubility of ketoprofen could be well observed in all loading concentration levels in all tested hydrogels. All ketoprofen loaded gels remained as monolithic dispersions. Since the ketoprofen was in a solid state inside the gel, it needed an additional step where it dissolved into the gel prior to diffusing into the upper layers of the gel, after which it could be released from the surface of the gel into the buffer.

Furthermore, it was observed after 6 hours, that the upper part of the ketoprofen loaded hydrogel nearer the exposed surface looked mostly transparent, while the lower section of the gel looked opaque white with precipitated drug inside. This indicates the possibility that the poor solubility of ketoprofen caused the drug to diffuse from the gel layer by layer, in contrast to drug diffusion evenly from the gel matrix, as was in the case of propranolol.

It was observed based on graphs 3 and 4 that when the same drug loading concentration was used, the observed released drug concentration was comparable with each other independent of the NFC hydrogel used. This observation indicates that the charge of the

ionized drug species and its possible interactions with different types of NFC hydrogel surface may not be a significant factor influencing the drug release from a NFC hydrogel. The solubility of the drug caused a more prominent difference in drug release.

The results obtained from the release study demonstrate that the wt. % released has linear correlation with time expressed in squareroots of seconds for both propranolol and ketoprofen loaded gels. Since for propranolol, the C_0 loaded in the NFC hydrogels was near or below the solubility of propranolol in water, and for ketoprofen the C_0 loaded in the NFC hydrogels was well above the solubility of ketoprofen in water, it can be said based on the results that the solubility of a drug does not seem to limit the usage of NFC hydrogels as a reservoir for drug release for the selected drugs. A precipitated drug may have a slight advantage (table 5) in controlled release applications, since the time point at which 60 wt. % was reached was more consistent for ketoprofen than for propranolol. Therefore the release of the precipitated drug may be slightly more predictable than for a dissolved drug.

It can be concluded that the NFC gel has potential as a drug reservoir for both cationic and anionic drug species. However, further modifications are necessary before the rate of release of the drugs from the gels is suitable for extended drug release applications.

12.2. Release study setup

In general, the setup for the release study was simple and it produced repeatable results. This setup had good points, which should be kept, and a few points for improvement, which should be considered for further studies in future. These are discussed below.

In the release study, the amount of drug loaded NFC hydrogel applied into the molds varied. The variation in weight of applied hydrogel varied between 0.46 and 8.96 %. However, this was fine, since the released amount from each parallel was compared with the original amount of drug available in each mold of each parallel set. Concerning the donor

compartment, it was observed that the diameter of the septum cap had robust value of 7.9 ± 0.0 mm, which was to be expected. The depth of the septum cap had more variation, with an average depth of 3.1 ± 0.2 mm. Therefore it can be concluded that the area exposed (0.49±0.00 cm^2) to drug release had a high and robust repeatability, which improve the comparability of the results obtained from the release tests.

Each of the release tests were run for a period of 6 hours. Concerning the durability of the gels, the gels did not start to flow and remained in their molds, as they should. It was noticed that for the anionic gels, it seemed that small parts of gel broke off from the surface and started to circulate within the beaker. This was noticeble by naked eye. However, it did not appear to affect the release profiles produced in general.

In the release study, there was no loaded gel version with a neutral drug carried out. Therefore, there are limited possibilities to evaluate the effect of the charge of the ionized drug species on the drug release from NFC hydrogel.

In addition, it is unknown what the pH values of the NFC hydrogels in HEPES buffer solution (pH 7.4) were, since these were not measured. Based on the information regarding the surface chemistry from literature review, and results from in pH measurements of unloaded NFC hydrogels in MilliQ water, it is possible that the hydrogels adjust to the surrounding pH environment.

The amount of drug released at the donor side exceeded 10 %. Therefore, no true sink conditions were maintained. Only at the receiver side, the drug concentration did not exceed 10 %. For more accurate estimations of P_{app} values, the experimental setup should be changed so that also at the donor side the amount of drug released from NFC hydrogel reservoir is kept under 10 %. This can be simply done by transferring the source at suitable time intervals into a fresh container.

12.3. Iontophoresis on skin

In both passive and active sets, the wt. %, which permeated through the skin, continued to increase after the electric current was stopped (graph 10). It can be observed from graph 11A and 11B that both current densities produce similar decreased enhancement after 5 hours of current application until the last point at 24 hours. However, it should be noted that only 2 data points were obtained to cover this time period. Therefore solid conclusions cannot be made for this part.

An enhancement factor of 170 has been reported for propranolol from a 5 % (m/v) solution under a current density of 0.5 mA/cm^2 applied through direct current iontophoresis for a duration of 12 hours in human skin *in vitro* (Jaskari et al. 2000). However, it should be noted that in this study, the epidermis was separated after placing the skin samples in +60 °C water for two minutes. Therefore, their result is not directly comparable with the result obtained in the experimental part of the current work. As stated in the results section, a clear difference between the two used current densities could not established, despite the high peak values of wt. % due to sudden permeation enhancement effect.

As it can be observed in graph 9, in both passive and active sets, during the 5 hour of DC current applications, the wt. % released did not reach over 1 %. At 24 hours (graph 10), less than 8 wt. % of drug had permeated through in all cases. Since the higher current density (0.50 mA/cm^2) is generally the highest acceptable value for human use, other options must be considered. Such options include addition of enhancement agents into the vehicle formulation or the synergistic use of other trandermal methods, such as ultrasound or microneedling, in conjunction with iontophoresis (Wang et al. 2005; Alexander et al. 2012).

It can be observed from results from the iontophoresis study, that the variation is greater when a biological skin tissue is part of the experimental system, in contrast to the release study. As mentioned in the literature review, the properties of *stratum corneum* are

influnced by gender and age in addition to its position in the body. There were no information regarding these details available for the porcine ears obtained. To gain a better understanding on the effects caused by biological variation, more parallel samples should be used.

Moreover, concerning enhanced permeability studies using iontophoresis, it should be investigated whether a temporary drug deposit is formed on the skin layers before an entrance into the dermal blood flow is realized, or if the depth of penetration is sufficient to allow the drug pass directly into the blood flow without any additional delay during the process of permeation through the skin layers.

Lastly, it should be noted, that there was a lack of a reference donor system present, for the comparison of the suitability of the NFC hydrogels as drug reservoirs in iontophoretic transdermal drug delivery. Also, the release study and the iontophoresis study were carried out in different termperature settings. The temperature might have affected the composition of NFC hydrogel during the higher temperature in addition to the electric stress induced by the iontophoresis. Therefore, more experimental work is required, before the assessment of the suitability of NFC hydrogels in iontophoretic transdermal drug delivery can be done.

12.4. Modelling

In general, the simulated and experimental data did not produce similar release profiles on a detailed level. For ketoprofen however, the simulated data seems to agree with the experimental data better at the loading concentration 90 mg/g in all three NFC hydrogels. An explanation for this may be the low ratio (< 0.33) released at 6 hours for these versions. Therefore, a decrease in the drug release rate is not seen.

It can be seen from graph 19, that both the area exposed for release and P_{app} can be changed to induce a different release profile of propranolol from NFC hydrogel A. The length of the mold does not have any affect on the release. For improvement of the results, further

experimental data needs to be obtained to improve the accuracy of the predictions made with simulations.

13. Conclusion

It was demonstrated in the experimental section of this Master's thesis that NFC hydrogels of birch origin exhibit a great potential as a reservoir for drug delivery. The drug loading can be done in a simple and efficient and the variation among samples is small. Both cationic and anionic drug species could be loaded and released from the tested NFC hydrogels. The release profiles obtained had linear correlation with the squareroot of time. However, for the controlled release, further modifications are required, especially if an extended drug release is desired. Further studies should be carried out in body temperature +37 °C and with neutral drug species for reference.

For the suitability accessment of the NFC hydrogels in iontophoretic transdermal drug delivery applications, further experiments should be carried out with different donor vehicles or solutions, in addition to the NFC hydrogels, to obtain reference values for the comparison of results. Based on this experimental work, the amount of drug permeating through could not be controlled by changing the current density applied. The simulation models did not represent experimental data in a detailed level. For improvement, more experimental data is required.

References

Alexander A, Dwivedi S, Ajazuddin, Giri TK, Saraf S, Saraf S, Tripathi, DK: Approaches for breaking the barriers of drug permeation through transdermal drug delivery. *J Control Release, 164*(1), 26-40, 2012.

Arora A, Prausnitz MR, Mitragotri S: Micro-scale devices for transdermal drug delivery. *Int J Pharm, 364*(2), 227-236, 2008.

Badiu D, Luque R, Rajendram R (2009). 123. Effect of Olive Oil on the Skin. In V. R. Preedy & R. R. Watson (Eds.), *Olives and Olive Oil in Health and Disease Prevention* (pp. 1125-1132): Elsevier, 2009.

Bhattacharya M, Malinen MM, Lauren P, Lou Y-R, Kuisma SW, Kanninen L, Lille M, Corlu A, GuGuen-Guillouzo C, Ikkala O, Laukkanen A, Urtti A, Yliperttula, M: Nanofibrillar cellulose hydrogel promotes three-dimensional liver cell culture. *J Control Release, 164*(3), 291-298, 2012.

Biniek K, Kaczvinsky J, Matts P, Dauskardt, RH: Understanding age-induced alterations to the biomechanical barrier function of human stratum corneum. *J Dermatol Sci*. *80(2)*, 94-101, 2015

Bouwstra JA, Honeywell-Nguyen PL, Gooris GS, Ponec M: Structure of the skin barrier and its modulation by vesicular formulations. *Prog Lipid Res, 42*(1), 1-36, 2003.

Bragd PL, Besemer AC, van Bekkum H: Bromide-free TEMPO-mediated oxidation of primary alcohol groups in starch and methyl α-d-glucopyranoside. *Carbohydr Res, 328*(3), 355-363, 2000.

Braverman IM: The Cutaneous Microcirculation. *J Investig Dermatol Symp Proc, 5*(1), 3-9, 2000.

Caspers PJ, Lucassen GW, Carter EA, Bruining HA, Puppels GJ: *In Vivo* Confocal Raman Microspectroscopy of the Skin: Noninvasive Determination of Molecular Concentration Profiles. *J Invest Dermatol, 116*(3), 434-442, 2001.

Choi J, Choi M-K, Chong S, Chung S-J, Shim C-K, Kim DD: Effect of fatty acids on the transdermal delivery of donepezil: *In vitro* and *in vivo* evaluation. *Int J Pharm, 422*(1–2), 83-90, 2012.

Choi MJ, Maibach HI: Role of Ceramides in Barrier Function of Healthy and Diseased Skin. *Am J Clin Dermatol, 6*(4), 215-223, 2005.

Curdy C, Kalia YN, Guy RH: Non-invasive assessment of the effects of iontophoresis on human skin in-vivo. *J Pharm Pharmacol, 53*(6), 769-777, 2001.

Das S, Subuddhi U: pH-Responsive guar gum hydrogels for controlled delivery of dexamethasone to the intestine. *Int J Biol Macromol, 79*, 856-863, 2015.

Delgado-Charro MB, Guy RH: Effective use of transdermal drug delivery in children. *Adv Drug Deliv Rev, 73*, 63-82, 2014.

DrugBank. DrugBank: Ketoprofen (DB01009). Retrieved on 11-Feb-2015, from http://www.drugbank.ca/drugs/DB01009, 2013a.

DrugBank. DrugBank: Propranolol (DB00571). Retrieved on 11-Feb-2015, from http://www.drugbank.ca/drugs/DB00571, 2013b.

Dubey S, Kalia YN: Electrically-assisted delivery of an anionic protein across intact skin: Cathodal iontophoresis of biologically active ribonuclease T1. *J Control Release, 152*(3), 356-362, 2011.

Dubey S, Kalia YN: Understanding the poor iontophoretic transport of lysozyme across the skin: When high charge and high electrophoretic mobility are not enough. *J Control Release, 183*(0), 35-42, 2014.

Elias PM, Gruber R, Crumrine D, Menon G, Williams ML, Wakefield JS, Holleran WM, Uchida Y: Formation and functions of the corneocyte lipid envelope (CLE). *BBA. Molecular and cell biology of lipids, 1841*(3), 314-318, 2014.

European Pharmacopoeia. *European Pharmacopoeia 8.0 Edition* (8.0 ed.). Strasbourg, France: EDQM, 2013.

Geerligs M, van Breemen L, Peters G, Ackermans P, Baaijens F, Oomens C: *In vitro* indentation to determine the mechanical properties of epidermis. *J Biomech, 44*(6), 1176-1181, 2011.

Gratieri T, Kalia YN: Targeted local simultaneous iontophoresis of chemotherapeutics for topical therapy of head and neck cancers. *Int J Pharm, 460*(1-2), 24-27, 2014.

Grimnes S, Martinsen ØG: Chapter 4 - Electrical properties of tissue. In the book *Bioimpedance and Bioelectricity Basics* (pp. 87-125), S Grimnes and Martinsen, ØG (Ed.), London: Academic Press, 2000.

Harpin V, Rutter N: Percutaneous alcohol absorption and skin necrosis in a preterm infant. *Arch Dis Child, 57*(6), 477-479, 1982.

Henry S, McAllister DV, Allen MG, Prausnitz MR: Microfabricated microneedles: A novel approach to transdermal drug delivery. *J Pharm Sci, 87*(8), 922-925, 1998.

Herkenne C, Naik A, Kalia YN, Hadgraft J, Guy RH: Pig ear skin *ex Vivo* as a model for *in Vivo* dermatopharmacokinetic studies in man. *Pharm Res, 23*(8), 1850-1856, 2006.

Jacobi U, Kaiser M, Toll R, Mangelsdorf S, Audring H, Otberg N, Sterry W, Lademann J: Porcine ear skin: an *in vitro* model for human skin. *Skin Res Technol, 13*(1), 19-24, 2007.

Jaskari T, Vuorio M, Kontturi K, Urtti A, Manzanares JA, Hirvonen J: Controlled transdermal iontophoresis by ion-exchange fiber. *J Control Release, 67*(2-3), 179-190, 2000.

Kalia YN, Naik A, Garrison J, Guy RH: Iontophoretic drug delivery. *Adv Drug Deliv Rev, 56*(5), 619-658, 2004.

Kikuchi S, Aosaki T, Bito K, Naito S, Katayama Y: *In vivo* evaluation of lateral lipid chain packing in human stratum corneum. *Skin Res Technol, 21*(1), 76-83, 2015.

Kitajima Y: Implications of normal and disordered remodeling dynamics of corneodesmosomes in stratum corneum. *Dermatologica Sinica, 33*(2), 58-63, 2015.

Klang V, Schwarz JC, Lenobel B, Nadj M, Auböck J, Wolzt M, Valenta C: In vitro vs. in vivo tape stripping: Validation of the porcine ear model and penetration assessment of novel sucrose stearate emulsions. *Eur J Pharm Biopharm, 80*(3), 604-614, 2012.

Klemm D, Kramer F, Moritz S, Lindström T, Ankerfors M, Gray D, Dorris A: Nanocelluloses: A New Family of Nature-Based Materials. *Angew Chem Int Ed Engl, 50*(24), 5438-5466, 2011.

Kolakovic R, Peltonen L, Laukkanen A, Hellman M, Laaksonen P, Linder MB, Hirvonen J, Laaksonen T: Evaluation of drug interactions with nanofibrillar cellulose. *Eur J Pharm Biopharm, 85*(3, Part B), 1238-1244, 2013.

Kolakovic R, Peltonen L, Laukkanen A, Hirvonen J, Laaksonen T: Nanofibrillar cellulose films for controlled drug delivery. *Eur J Pharm Biopharm, 82*(2), 308-315, 2012.

Kotzki S, Roustit M, Arnaud C, Godin-Ribuot D, Cracowski J-L: Effect of continuous vs pulsed iontophoresis of treprostinil on skin blood flow. *Eur J Pharm Sci, 72*, 21-26, 2015.

Lau WM, Ng KW, Sakenyte K, Heard CM: Distribution of esterase activity in porcine ear skin, and the effects of freezing and heat separation. *Int J Pharm, 433*(1–2), 10-15, 2012.

Leyva-Mendivil MF, Page A, Bressloff NW, Limbert G: A mechanistic insight into the mechanical role of the stratum corneum during stretching and compression of the skin. *J Mech Behav Biomed Mater, 49*, 197-219, 2015.

Liao F, Burns S, Jan Y-K: Skin blood flow dynamics and its role in pressure ulcers. *J Tissue Viability, 22*(2), 25-36, 2013.

Lin C-C, Metters AT: Hydrogels in controlled release formulations: Network design and mathematical modeling. *Adv Drug Deliv Rev, 58*(12–13), 1379-1408, 2006.

Lou Y-R, Kanninen L, Kuisma T, Niklander J, Noon LA, Burks D, Urtti A, Yliperttula M: The Use of Nanofibrillar Cellulose Hydrogel As a Flexible Three-Dimensional Model to Culture Human Pluripotent Stem Cells. *Stem Cells Dev, 23*(4), 380-392, 2014.

Luebberding S, Krueger N, Kerscher M: Skin physiology in men and women: in vivo evaluation of 300 people including TEWL, SC hydration, sebum content and skin surface pH. *Int J Cosmet Sci, 35*(5), 477-483, 2013.

MacNeil S: Biomaterials for tissue engineering of skin. *Mater Today (Kidlington), 11*(5), 26-35, 2008.

Malinovskaja K, Laaksonen T, Hirvonen J: Controlled transdermal delivery of leuprorelin by pulsed iontophoresis and ion-exchange fiber. *Eur J Pharm Biopharm, 88*(3), 594-601, 2014.

Malinovskaja K, Laaksonen T, Kontturi K, Hirvonen J: Ion-exchange and iontophoresis-controlled delivery of apomorphine. *Eur J Pharm Biopharm, 83*(3), 477-484, 2013.

Maloney TC: Network swelling of TEMPO-oxidized nanocellulose. *Holzforschung, 69*(2), 207-213, 2015.

Marro D, Guy RH, Delgado-Charro MB: Characterization of the iontophoretic permselectivity properties of human and pig skin. *J Control Release, 70*(1–2), 213-217, 2001.

Menon GK, Cleary GW, Lane ME: The structure and function of the stratum corneum. *Int J Pharm, 435*(1), 3-9, 2012.

Oshizaka T, Kikuchi K, Kadhum WR, Todo H, Hatanaka T, Wierzba K, Sugibayashi K: Estimation of skin concentrations of topically applied lidocaine at each depth profile. *Int J Pharm, 475*(1–2), 292-297, 2014.

Pönni R, Pääkkönen T, Nuopponen M, Pere J, Vuorinen T: Alkali treatment of birch kraft pulp to enhance its TEMPO catalyzed oxidation with hypochlorite. *Cellulose (Lond), 21*(4), 2859-2869, 2014.

Prausnitz MR: The effects of electric current applied to skin: A review for transdermal drug delivery. *Adv Drug Deliv Rev, 18*(3), 395-425, 1996.

Prausnitz MR, Mitragotri S, Langer R: Current status and future potential of transdermal drug delivery. *Nat Rev Drug Discov, 3*(2), 115-124, 2004.

Rowland M, Tozer T: *Clinical Pharmacokinetics and Pharmacodynamics: Concepts and Applications* (4th ed.). Philadelphia, USA: Lippincott Williams & Wilkins, 2011.

Sacui IA, Nieuwendaal RC, Burnett DJ, Stranick SJ, Jorfi M, Weder C, Foster EJ, Olsson RT, Gilman JW: Comparison of the Properties of Cellulose Nanocrystals and Cellulose Nanofibrils Isolated from Bacteria, Tunicate, and Wood Processed Using Acid, Enzymatic, Mechanical, and Oxidative Methods. *ACS Appl Mater Interfaces, 6*(9), 6127-6138, 2014.

Saltzman WM: *Drug delivery: engineering principles for drug delivery*, Oxford University Press, Inc, New York, 2001.

Saluja S, Kasha PC, Paturi J, Anderson C, Morris R, Banga AK: A novel electronic skin patch for delivery and pharmacokinetic evaluation of donepezil following transdermal iontophoresis. *Int J Pharm, 453*(2), 395-399, 2013.

Siepmann J, Peppas NA: Modeling of drug release from delivery systems based on hydroxypropyl methylcellulose (HPMC). *Adv Drug Deliv Rev, 48*(2–3), 139-157, 2001.

Siepmann J, Siepmann F: Modeling of diffusion controlled drug delivery. *J Control Release, 161*(2), 351-362, 2012.

Siró I, Plackett D: Microfibrillated cellulose and new nanocomposite materials: a review. *Cellulose (Lond), 17*(3), 459-494, 2010.

Tesselaar E, Sjöberg F: Transdermal iontophoresis as an *in-vivo* technique for studying microvascular physiology. *Microvasc Res, 81*(1), 88-96, 2011.

Toyoda M, Hama S, Ikeda Y, Nagasaki Y, Kogure K: Anti-cancer vaccination by transdermal delivery of antigen peptide-loaded nanogels via iontophoresis. *Int J Pharm, 483*(1–2), 110-114, 2015.

Tratta E, Pescina S, Padula C, Santi P, Nicoli S: *In vitro* permeability of a model protein across ocular tissues and effect of iontophoresis on the transscleral delivery. *Eur J Pharm Biopharm, 88*(1), 116-122, 2014.

Valo H, Arola S, Laaksonen P, Torkkeli M, Peltonen L, Linder MB, Serimaa R, Kuga S, Hirvonen J, Laaksonen T: Drug release from nanoparticles embedded in four different nanofibrillar cellulose aerogels. *Eur J Pharm Sci, 50*(1), 69-77, 2013.

van der Geest R, Elshove DAR, Danhof M, Lavrijsen APM, Bodde HE: Non-invasive assessment of skin barrier integrity and skin irritation following iontophoretic current application in humans. *J Control Release, 41*(3), 205-213, 1996.

van Logtestijn MDA, Dominguez-Hüttinger E, Stamatas GN, Tanaka RJ: Resistance to water diffusion in the stratum corneum is depth-dependent. *PloS one, 10*(2), e0117292, 2015.

Volpato NM, Nicoli S, Laureri C, Colombo P, Santi P: In vitro acyclovir distribution in human skin layers after transdermal iontophoresis. *J Control Release, 50*(1–3), 291-296, 1998.

Wang Y, Thakur R, Fan Q, Michniak B: Transdermal iontophoresis: combination strategies to improve transdermal iontophoretic drug delivery. *Eur J Pharm Biopharm, 60*(2), 179-191, 2005.

Wesley NO, Maibach HI: Racial (Ethnic) Differences in Skin Properties. *Am J Clin Dermatol, 4*(12), 843-860, 2003.

Wiedersberg S, Guy RH: Transdermal drug delivery: 30 + years of war and still fighting! *J Control Release, 190*, 150-156, 2014.

Appendices

Appendix A: ANOVA data analysis for the iontophoresis study

Anova: Single Factor

SUMMARY

Groups	*Count*	*Sum*	*Average*	*Variance*
Column 1	10	8.342256	0.834226	4.506629
Column 2	10	7.678967	0.767897	3.236475

ANOVA

Source of Variation	*SS*	*df*	*MS*	*F*	*P-value*	*F crit*
Between Groups	0.021998	1	0.021998	0.005682	0.940745	4.413873
Within Groups	69.68793	18	3.871552			
Total	69.70993	19				

Appendix B: Equations for Stella models

1. Model structure for propranolol release simulation

amount_of_propranolol_available_for_release_in_gel(t) =
amount_of_propranolol_available_for_release_in_gel(t - dt) + (-diffusion_from_gel) * dt
INIT amount_of_propranolol_available_for_release_in_gel = amount_of_drug_available
OUTFLOWS:
diffusion_from_gel = mass_over_mass_concentration_of_propranolol_in_gel * CL
released_from_gel(t) = released_from_gel(t - dt) + (diffusion_from_gel) * dt
INIT released_from_gel = 0
INFLOWS:
diffusion_from_gel = mass_over_mass_concentration_of_propranolol_in_gel * CL
amount_of_drug_available = av_weight_of_propranolol_loaded_gel_applied *
original_C_of_loaded_gel__10_mg_over_g
Area = 0.490166994
av_weight_of_propranolol_loaded_gel_applied = 0.132233333
CL = Papp_from_10to60minPinA10data * Area
D = IF Mt_over_Minf_simulated = 0 then 0
else (Mt_over_Minf_simulated^2*PI*0.32^2)/(16*time)
L0 = 0.31
mass_over_mass_concentration_of_propranolol_in_gel =
amount_of_propranolol_available_for_release_in_gel /
av_weight_of_propranolol_loaded_gel_applied
Mt_over_Minf_based__math_equation = 4 * ((D * time) / (PI * L0^2))^(0.5)
Mt_over_Minf_simulated = released_from_gel / amount_of_drug_available
original_C_of_loaded_gel__10_mg_over_g = 11.27798019
Papp_from_10to60minPinA10data = 2.4976*10^(-5)*60*60

---

2. Model for propranolol release simulation, with experimental density

amount_of_propranolol_available_for_release_in_gel(t) =
amount_of_propranolol_available_for_release_in_gel(t - dt) + (-diffusion_from_gel) * dt
INIT amount_of_propranolol_available_for_release_in_gel = amount_of_drug_available
OUTFLOWS:
diffusion_from_gel = mg_over_ml_concentration_of_propranolol_in_gel * CL
released_from_gel(t) = released_from_gel(t - dt) + (diffusion_from_gel) * dt
INIT released_from_gel = 0
INFLOWS:
diffusion_from_gel = mg_over_ml_concentration_of_propranolol_in_gel * CL

amount_of_drug_available = av_weight_of_propranolol_loaded_gel_applied * original_C_of_loaded_gel__10_mg_over_g
Area = 0.490166994
av_weight_of_propranolol_loaded_gel_applied = 0.132233333
CL = Papp_from_10to60minPinA10data * Area
D = IF Mt_over_Minf_simulated = 0 then 0
else (Mt_over_Minf_simulated^2*PI*0.32^2)/(16*time)
exp_dens = 0.895020846
L0 = 0.31
mg_over_ml_concentration_of_propranolol_in_gel = amount_of_propranolol_available_for_release_in_gel / v
Mt_over_Minf_based__math_equation = 4 * ((D * time) / (PI * L0^2))^(0.5)
Mt_over_Minf_simulated = released_from_gel / amount_of_drug_available
original_C_of_loaded_gel__10_mg_over_g = 11.27798019
Papp_from_10to60minPinA10data = 2.4976*10^(-5)*60*60
v = av_weight_of_propranolol_loaded_gel_applied / exp_dens

---

3. Model for ketoprofen release simulation

Minf(t) = Minf(t - dt) + (-diffusion_from_gel) * dt
INIT Minf = amount_of_drug_available
OUTFLOWS:
diffusion_from_gel = mass_over_mass_concentration_of_ketoprofen_in_gel * CL
Mt(t) = Mt(t - dt) + (diffusion_from_gel) * dt
INIT Mt = 0
INFLOWS:
diffusion_from_gel = mass_over_mass_concentration_of_ketoprofen_in_gel * CL
amount_of_drug_available = av_weight_of_ketoprofen_loaded_gel_applied * Cini_of_loaded_gel_10_mg_over_g
Area = 0.490166994
av_weight_of_ketoprofen_loaded_gel_applied = 0.132156667
Cini_of_loaded_gel_10_mg_over_g = 9.922183987
CL = Papp_from_ketoprofen_data_KinA10_20to150 * Area
D = IF Mt=0 then 0
ELSE (Mt/Area)^2 * (1 / (solubility_of_ketoprofen_in_water * (2*Cini_of_loaded_gel_10_mg_over_g - solubility_of_ketoprofen_in_water) * time))
mass_over_mass_concentration_of_ketoprofen_in_gel = Minf / av_weight_of_ketoprofen_loaded_gel_applied
Mt_over_Minf_math_equation = (Area / amount_of_drug_available) * SQRT(D * solubility_of_ketoprofen_in_water * 2 *Cini_of_loaded_gel_10_mg_over_g * time)
Mt_over_Minf_simulated = Mt / amount_of_drug_available
Papp_from_ketoprofen_data_KinA10_20to150 = (1.2128e-05)*60*60

solubility_of_ketoprofen_in_water = 0.051

---

4. Model for ketoprofen release simulation, with experimental density

Minf(t) = Minf(t - dt) + (-diffusion_from_gel) * dt
INIT Minf = amount_of_drug_available
OUTFLOWS:
diffusion_from_gel = mg_over_ml_concentration_of_ketoprofen_in_gel * CL
Mt(t) = Mt(t - dt) + (diffusion_from_gel) * dt
INIT Mt = 0
INFLOWS:
diffusion_from_gel = mg_over_ml_concentration_of_ketoprofen_in_gel * CL
amount_of_drug_available = av_weight_of_ketoprofen_loaded_gel_applied * Cini_of_loaded_gel_10_mg_over_g
Area = 0.490166994
av_weight_of_ketoprofen_loaded_gel_applied = 0.132156667
Cini_of_loaded_gel_10_mg_over_g = 9.922183987
CL = Papp_from_ketoprofen_data_KinA10_20to150 * Area
D = IF Mt=0 then 0
ELSE (Mt/Area)^2 * (1 / (solubility_of_ketoprofen_in_water * (2*Cini_of_loaded_gel_10_mg_over_g - solubility_of_ketoprofen_in_water) * time))
exp_dens = 0.895020846
mg_over_ml_concentration_of_ketoprofen_in_gel = Minf / v
Mt_over_Minf_math_equation = (Area / amount_of_drug_available) * SQRT(D * solubility_of_ketoprofen_in_water * 2 *Cini_of_loaded_gel_10_mg_over_g * time)
Mt_over_Minf_simulated = Mt / amount_of_drug_available
Papp_from_ketoprofen_data_KinA10_20to150 = (1.2128e-05)*60*60
solubility_of_ketoprofen_in_water = 0.051
v = av_weight_of_ketoprofen_loaded_gel_applied /exp_dens

---

5. Model for iontophoretic transdermal permeation simulation (both passive and active)

Minf(t) = Minf(t - dt) + (-diffusion_across_skin) * dt
INIT Minf = amount_of_drug_available
OUTFLOWS:
diffusion_across_skin = mass_over_mass_concentration_of_propranolol_in_gel * CL
Mt(t) = Mt(t - dt) + (diffusion_across_skin) * dt
INIT Mt = 0
INFLOWS:
diffusion_across_skin = mass_over_mass_concentration_of_propranolol_in_gel * CL
amount_of_drug_available = Cini_of_PinA30_at_donor_side * av_weight_of_propranolol_loaded_gel_applied

Area_available_in_iontoph = 2.378552158
av_weight_of_propranolol_loaded_gel_applied = 1.029
Cini_of_PinA30_at_donor_side = 34.06862715
CL = papp025ion_180to300min * Area_available_in_iontoph
exp_dens = 0.895020846
mass_over_mass_concentration_of_propranolol_in_gel = Minf / v
Mt_over_Moriginal = Mt / amount_of_drug_available
papp025ion_180to300min = (2.61442E-07)*60*60
v = av_weight_of_propranolol_loaded_gel_applied / exp_dens
